

LIBRARY Michigan State University

This is to certify that the dissertation entitled

Effect of Various Oxyanions of Nitrogen on Corrosion Inhibition of Aluminum Alloy

presented by
Hyung-Joon Kim

has been accepted towards fulfillment of the requirements for

Ph.D. degree in Metallurgy

A gleet Scenure

Major professor

Date 19 March 1987

MSU is an Affirmative Action/Equal Opportunity Institution

0-12771



RETURNING MATERIALS: Place in book drop to remove this checkout from your record. FINES will be charged if book is returned after the date

stamped below.

MAR 2 1 1996

EFFECT OF VARIOUS OXYANIONS OF NITROGEN ON CORROSION INHIBITION OF ALUMINUM ALLOY

By

Hyung-Joon Kim

A DISSERTATION

Submitted to

Michigan State University
in partial fulfillment of the requirements
for the degree of

DOCTOR OF PHILOSOPHY

Department of Metallurgy, Mechanics and Materials Science

ABSTRACT

EFFECT OF VARIOUS OXYANIONS OF NITROGEN
ON CORROSION INHIBITION OF ALUMINUM ALLOY

Ву

Hyung-Joon Kim

Potentiodynamic polarization was used to evaluate inhibitor effectiveness for AA 7075-T6 in solutions containing chloride, at varying temperatures.

Inhibitors included various anions of nitrogen and boron, and ammonium ion. Generally, passivation was found in distilled water. In the presence of chloride, however, passivity depends on inhibitor concentration. Inhibitive efficiency of nitrogen oxyanions, based on the pitting potential, is in the decreasing order of: $N_2O_2^- > NH_4^+ > NO_3^- > Combination of NO_2^-$ with $B_4O_7^{2-} > NO_2^-$.

Current density depends logarithmically on temperature in solutions of sodium nitrite and sodium nitrate; the activation energies are 2.68 kcal/mol and 4.88 kcal/mol, respectively.

Acknowledgments

I would like to express my deepest gratitute and appreciation to Dr. Robert Summitt who as major professor provided direction and encouragement throughout the course of this study and in preparation of this manuscript.

I also wish to thank the other members of my guidance committee, Dr. K. Mukherjee, Dr. G. Gottstein and Dr. H. Eick for their inspiration.

Thanks are extended to U.S. Air Force and U.S. Office of Naval Research and the Department of Metallurgy, Mechanics and Materials Science at Michigan State University for financial support during the doctoral program.

Finally, I would like to especially thank my parents, uncle and wife (Young-Joo) for their encouragement and understanding.



TABLE OF CONTENTS

LIST	OF TABLES	V
LIST	OF FIGURES	vi
I.	INTRODUCTION	1
II.	THEORETICAL BACKGROUND AND LITERATURE REVIEW	3
	A. THEORY OF PASSIVITY	3
	B. ELECTROCHEMISTRY OF PASSIVATION	6
	C. INHIBITION	12
	D. NITROGEN OXYANIONS	31
	E. RESEARCH PROGRAM	43
III.	EXPERIMENTAL TEST PROCEDURE AND APPARATUS	44
	A. EXPERIMENTAL SYSTEM	44
	B. EXPERIMENTAL TECHNIQUE	51
	C. 7075-T6 AL ALLOY HANDLING, CLEANING AND TEST	
	SOLUTION	54
IV.	EXPERIMENTAL RESULTS	61
	A. DISTILLED WATER AND SODIUM CHLORIDE	61
	B. EFFECTS OF INHIBITORS	61
	C. EFFECTS OF TEMPERATURE	82

V. DISCUSSION	••••••	88
VI. CONCLUSION	••••••	109
REFERENCES		110

LIST OF TABLES

Table		Page
1.	The Oxyanions of Nitrogen	32
2.	Oxidation Potential Data for Reduction of	
	Nitrate Ion	37
3.	Chemical Composition	55
4.	Mechanical Properties of 7075-T6 Al Alloys	55
5.	The Test Solution	57
6.	Lynch Formulation	58
7.	Pitting Potential of Different Test Solutions	
	With 0.1 wt.% NaCl	100

LIST OF FIGURES

Figure	e	Page
1.	Schematic Structure of Passive Film	. 7
2.	The Corrosion Diagram of Evans	. 8
3.	Electronic Structure of NO ₂	. 34
4.	Electronic Structure of NO ₃	. 36
5.	Electronic Structure of N ₂ O ₂ ²⁻	. 40
6.	The Experimental System	. 46
7.	The Corrosion Cell	. 49
8.	The Anodic Polarization of 7075-T6 Al Alloy in	
	Dilute Solution	. 62
9.	The Anodic Polarization of 7075-T6 Al Alloy in	
	0.1 wt.% Sodium Chloride	. 63
10.	The Anodic Polarization of 7075-T6 Al Alloy in	
	Sodium Nitrite	. 65
11.	The Effect of Concentrations of Nitrite on	
	Current Density at Constant Potential	. 66



12.	The Anodic Polarization of 7075-T6 Al Alloy in	
	Sodium Nitrite with Sodium Chloride	67
13.	The Anodic Polarization of 7075-T6 Al Alloy in	
	Sodium Nitrite and Borax	68
14.	The Anodic Polarization of 7075-T6 Al Alloy in	
	Sodium Nitrite and Borax with Sodium Chloride	69
15.	The Anodic Polarization of 7075-T6 Al Alloy in	
	Lynch Formulation	71
16.	The Anodic Polarization of 7075-T6 Al Alloy in	
	Lynch Formulation with Sodium Chloride	72
17.	The Cathodic Polarization of 7075-T6 Al Alloy in	
	Sodium Nitrite	73
18.	The Cathodic Polarization of 7075-T6 Al Alloy in	
	Sodium Nitrite with Sodium Chloride	74
19.	The Anodic Polarization of 7075-T6 Al Alloy in	
	Sodium Nitrate	76
20.	The Anodic Polarization of 7075-T6 Al Alloy in	
	Sodium Nitrate with Sodium Chloride	77
21.	The Effect of Concentrations of Nitrate on	
	Current Density at Constant Potential	78



22.	The Anodic Polarization of 7075-T6 Al Alloy in	
	Sodium Hyponitrite	80
23.	The Anodic Polarization of 7075-T6 Al Alloy in	
	Sodium Hyponitrite with Sodium Chloride	81
24.	The Anodic Polarization of 7075-T6 Al Alloy in	
	Ammonium Hydroxide	83
25.	The Anodic Polarization of 7075-T6 Al Alloy in	
	Ammonium Hydroxide with Sodium Chloride	84
26.	The Anodic Polarization of 7075-T6 Al Alloy in	
	Sodium Nitrite vs. Temperature	85
27.	The Anodic Polarization of 7075-T6 Al Alloy in	
	Sodium Nitrate vs. Temperature	86
28.	Schematic Models of the Passive Film	94
29.	Schematic Polarization Diagram for Oxidizing	
	Inhibitor	97
30.	Dependence of the Current Density on Temperature	
	in Sodium Nitrate	105
31.	Dependence of the Current Density on Temperature	
	in Codium Nitrito	106

I. Introduction

This study is an experimental exploration of the relations between the inhibitor/accelerant properties and the electrochemistry in 7075-T6 Al alloy. A potentiodynamic polarization technique is used to evaluate the effectiveness of inhibitor when 7075-T6 high-strength aluminum alloy is exposed to solutions with and without chloride ions. Nitrite, nitrate, hyponitrite and ammonium hydroxide are used as the inhibitors.

Aluminum has a notable resistance to corrosion, which is remarkable from the viewpoint of its high free-energy content which would suggest a powerful tendency to corrosion. In fact, a free aluminum surface corrodes rapidly and soon is covered by a thin protective oxide film that makes the metal immune to further corrosion. The corrosion resistance, therefore, depends upon the resistance of the oxide film to attack, that is, upon the degree of passivity. In practice, the corrosion behavior of aluminum is determined mainly by the behavior of the oxide-covered metal surface towards the corroding medium, which behavior is very dependent on the nature of the anion in solution. In nearneutral air-saturated solutions, the corrosion of aluminum is generally inhibited by the same anions which are inhibitive for iron, e.g., chromate, phosphate, and acetate. Aggressive anions for aluminum include the halide ions, i.e., F, Br, Cl, and I, which cause pitting attack; and

anions which form soluble complexes with aluminum, e.g., citrate and tartrate which cause general attack. In the presence of chloride ions, the breakdown of passivating oxide films results from the severe pitting of the underlying metal. Competitive effects are observed in the action of mixtures of inhibitive anions and chloride ions on aluminum.

Generally, the results show that the corrosion of aluminum depends on the nature of passivity, which in turn is determined by the specific anions present in the solution.

II. Theoretical Background and Literature Review

A. Theory of Passivity

The protection of metals against corrosion in the environment can be enhanced with inhibitors. When the inhibition is obtained with the compounds altering mainly the kinetics of anionic reaction -- this mechanism being most effective in neutral electrolytes --, inhibition is closely related to the passivation.

The major theories of passivity are divided into four categories: a) metal modification; b) reaction rate; c) oxide film; d) adsorption.

a) Metal-Modification Theories

Schonbein⁽¹⁾ considered that the passive and active states of iron might represent allotropic modifications of the metal. Finklestein⁽²⁾ supported a metal-modification theory by proposing the valence theory of passivity, where the metallic iron is made up of a mixture of Fe²⁺ and Fe³⁺ ions, with passive iron consisting mostly of Fe³⁺ and active iron consisting mostly of Fe²⁺, i.e., equilibrium exists between allotropic forms of the metal, i.e., Fe²⁺, Fe³⁺, and electrons⁽³⁾. Metal-modification theories are no longer of serious interest except in the modern counterpart

longer of serious interest except in the modern counterpart as a guide to establish the kind of surface films that form application of electronic configuration to transition metals.

b) Reaction-Velocity Theory

According to this theory⁽⁴⁾, the passive state results from a slow rate of metal dissolution independent of any surface film. The slow reactivity leads to sluggish hydration of anhydrous ions in the metal lattice, hydration being necessary to ion solubility in an aqueous environment. This slow reactivity easily accounts for the marked anodic polarization characteristic of passivated metal. This theory, however, is expressed in part by the present adsorption theory. The chemisorbed oxygen film results from a displacement of adsorbed H₂O molecules with a consequent reduction in rate of metal-ion hydration, or metal-complex formation necessary for the solubility of such ions in water; or, the surface electrical double layer is altered in composition and structure by adsorbed oxygen resulting similarly in a reduced reaction rate.

c) Oxide Film Theory

An oxide model for passive film was proposed by $Gmelin^{(5)}$, $Haber^{(6)}$, $Heathcote^{(7)}$, $Evans^{(8)}$. Flade suggested that an oxide film or an oxygen alloy layer at the

metal surface was a possible cause of passivity. Also, it is known that a protective oxide film is the passive film on metals such as Cr, Ni, Ti, Al, Mo, etc.. Often, no distinction is made between oxide films and adsorbed films, both kinds being considered to isolate similarly the metal from its environment. But the distinction should be made because the mechanism of protection by adsorbed films relates to retarded surface reaction rates rather than to retarded diffusion rates through oxides supposedly making up the passive layer as explained with the oxide film theory.

d) Adsorption Theory

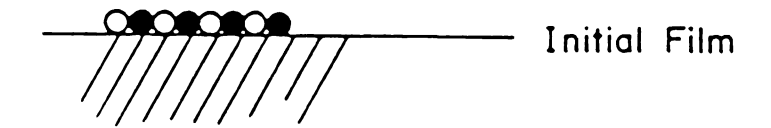
It is proposed by Fredenhagen⁽⁹⁾ that the passive film on Fe consists of oxygen that satisfies chemical affinities of the surface and, hence, results in reduced reactivity. Langmuir⁽¹⁰⁾ suggested that his measurements showed that oxygen adsorbed on tungsten exhibited reduced chemical reactivity compared with oxygen in the oxide WO₃, and that the well-known passive properties of Cr were probably related to a similar film of adsorbed oxygen. On progressive anodic polarization of a metal to more noble potentials, multilayer adsorption of oxygen builds up the passive film thickness. The pronounced negative charge of adsorbed oxygen attracts and slowly incorporates into the film in nonstoichiometric amounts positively charged metal ions, as well as protons from the aqueous environment⁽¹¹⁾.

The proton comes from the presence of H_2O or H in passive films on $Fe^{(12)}$, (13) and on stainless steels (14). It is reported that the mixed adsorbed oxygen-metal-hydrogen (O-M-H) passive film can account for the observation that passivity results from less than monolayer amounts of oxygen on the surface (15).

In summary, the most promising model for the passive film on metals is one made up of adsorbed oxygen containing metal ions and protons, in indefinite proportions, and including the category of nonstoichiometric oxides (Figure 1). The latter designation is applicable to passive films on such metals as Al, Ta, and Zr, etc.

B. Electrochemistry of passivation

Figure 2 shows the corrosion diagram of Evans represented by two curves, a cathodic-polarization curve CB and an anodic polarization curve AB, that characterize the dependence of the cathode and anode potentials on the current strength. The intersection point of the curves corresponds to the maximum current I_{max} . The measure of control for the corrosion rate of the given electrode reaction is determined by the slope of the curves, i.e., the tangents of angles α and β for the cathodic and anodic reactions, respectively. Thus the cathodic and anodic potentials are given by



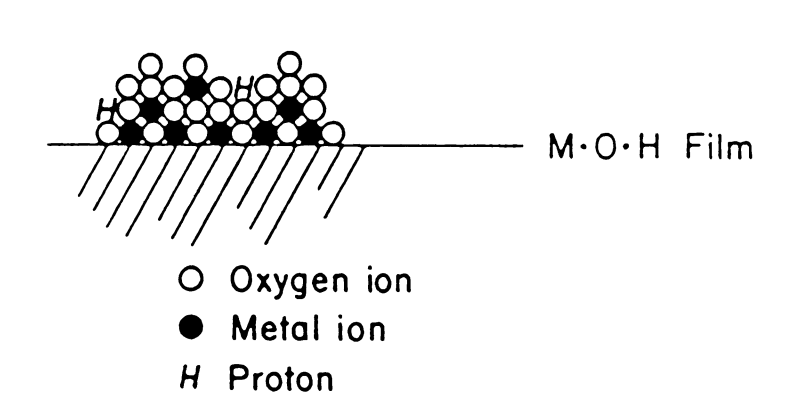


Figure 1. Schematic Structure of Initial Passive Film containing less than monolayer amounts of adsorbed oxygen, and of a thicker passive film containing additional metal ions and protons in nonstoichiometric amounts.



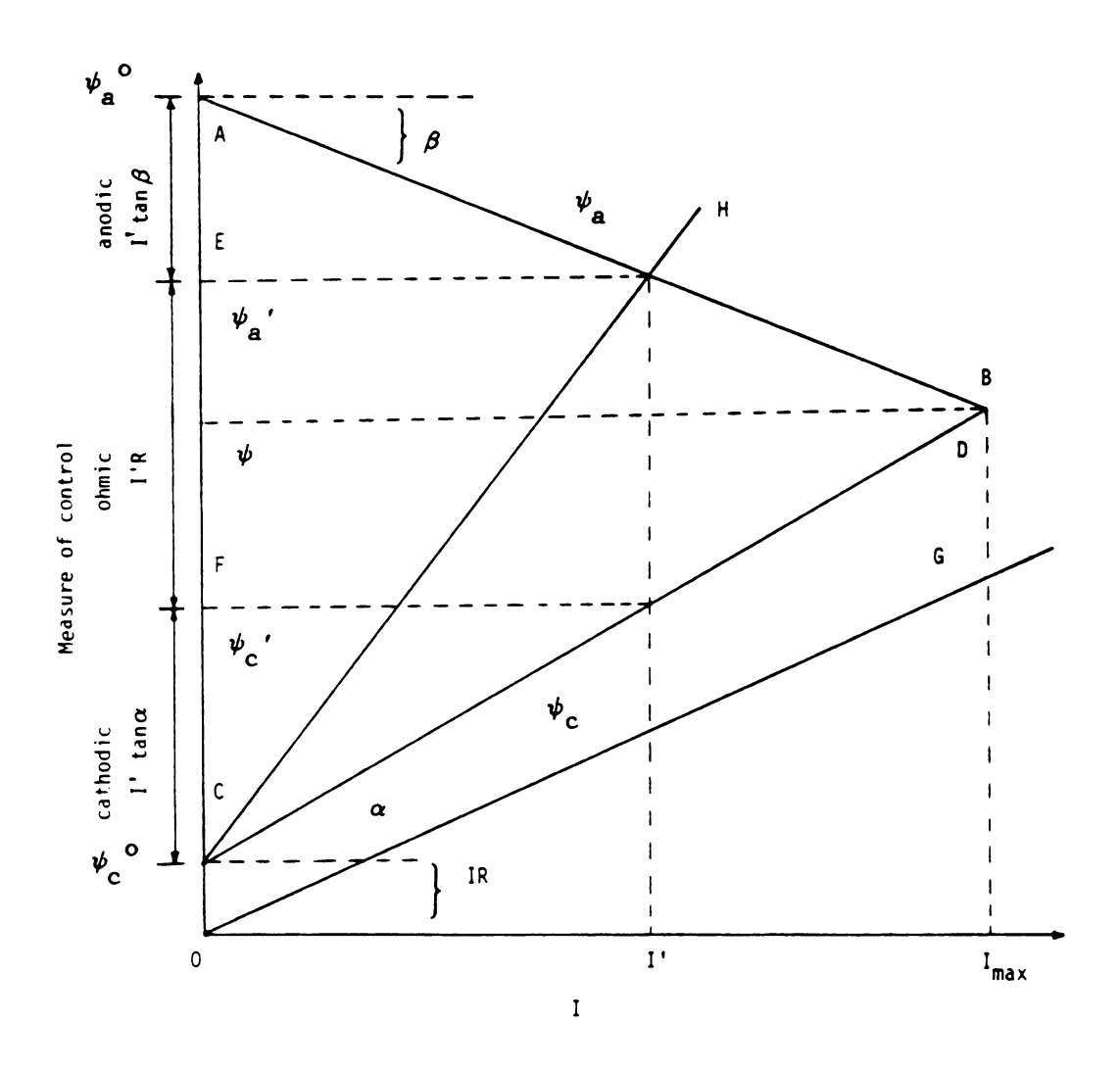


Figure 2. The Corrosion Diagram of Evans.

$$\psi_{c} = \psi_{c}^{\circ} - I \cdot \tan \alpha = \psi_{c}^{\circ} + P_{c} \cdot I$$
 (1)

$$\psi_{a} = \psi_{a}^{O} + I \cdot \tan \beta = \psi_{a}^{O} + P_{a} \cdot I, \qquad (2)$$

where P_c and P_a are the cathodic and anodic polarization resistances.

The cathode and anode potential are equal at the point of intersection of the curves corresponding to the maximum current:

$$\psi_{c}^{o} - P_{c} \cdot I_{max} = \psi_{a}^{o} + P_{a} \cdot I_{max}$$
 (3)

$$I_{\text{max}} = (\psi_{c}^{0} - \psi_{a}^{0})/(P_{a} + P_{c}).$$
 (4)

Taking into account the ohmic potential drop in the electrolyte (I'R), the current I' corresponding to the ohmic resistance R is

$$I' = (\psi_c' - \psi_a')/R.$$
 (5)

Thus,

$$\psi_{a}' = \psi_{a}^{ O} + P_{a} \cdot I', \qquad (6)$$

$$\psi_{c}' - \psi_{c}' - P_{c} \cdot I'. \tag{7}$$

Consequently,

$$I' = (\psi_c^0 - \psi_a^0)/(R + P_c + P_a). \tag{8}$$



Equation (8) is the fundamental equation describing the corrosion process, taking into account both the polarization resistance and the ohmic resistance. The current can be determined by the initial potential difference and by the sum of the polarization and ohmic resistance.

From Equations (1) and (2), the equations of the cathodic and anodic polarization curve are modified as

$$\psi_{c} = \psi_{c}^{o} - K_{1} \cdot (I/F_{c}), \text{ and}$$
 (9)

$$\psi_a = \psi_a^o + K_2 \cdot (I/F_a),$$
 (10)

where ${\bf K}_1$ and ${\bf K}_2$ are the polarizability constants of the cathode and anode at unit current density, and ${\bf F}_{\bf C}$ and ${\bf F}_{\bf a}$ are the areas of the passive (cathode) and active (anode) parts of the electrodes. The intensity of the corrosion current of the system, defined as the rate of the corrosion process calculated per unit surface area subjected to corrosion damage, is determined by the equation

$$I - (\psi_c^o - \psi_a^o)/[R + (K_1/F_c) + (K_2/F_a)].$$
 (11)

When an inhibitor impedes only the anodic process, the corrosion rate may decrease either because of a lower rate of metal ion transfer into solution as a result of adsorption of positively charged particles in the double layer,



or because of a contraction of the active part of the electrode as a result of passivation. It can be shown that an anodic inhibitor contracts the active part of the electrode considerably more than it reduces the corrosion current. For a completely polarized system, R is small in comparison with the polarization resistance. From Equation (11),

$$I = (\psi_c^o - \psi_a^o)/[(K_1/F_c) + (K_2/F_a)]$$
$$= \Delta \psi/[(K_1/F_c) + (K_2/F_a)].$$
(12)

The corrosion current in the initial electrolyte is

$$I_1 - \Delta \psi_1 / [(K_1/F_{c1}) + (K_2/F_{a1})].$$
 (13)

The corrosion current in the electrolyte containing the inhibitor is

$$I_2 - \Delta \psi_2 / [(K_1/F_{c2} + (K_2/F_{a2})].$$
 (14)

On the condition that $\Delta\psi_1$ - $\Delta\psi_2$ and K_1 = K_2 , the following can be obtained, from F_{a1} + F_{C1} = 1 and F_{a2} + F_{C2} = 1,

$$F_{a1}/F_{a2} = (I_1/I_2)(F_{c2}/F_{c1}).$$
 (15)

Since F_{C2} > F_{C1},

$$F_{a1}/F_{a2} > I_1/I_2.$$
 (16)

From Equation (16), it can be seen that the active part of the electrode in the presence of an inhibitor contracts more strongly than the corrosion current is reduced.

C. Inhibition

Shreir (16) notes that organic compounds, particularly those containing elements of Group V and VI of the Periodic Table, such as nitrogen, phosphorus, arsenic, oxygen, sulfur and selenium are effective inhibitors in aqueous acid solutions. Generally, the primary step in the action of inhibitors in acid solutions is its adsorption onto the metal surface, which usually is oxide free. Then the adsorbed inhibitor acts to retard the cathodic and/or anodic electrochemical process of the corrosion.

The corrosion of metals in neutral solutions differs from that in acid solutions in two important respects. In air-saturated solutions, the main cathodic reaction in neutral solutions is the reduction of dissolved oxygen, whereas in acid solution, it is hydrogen evolution. Corroding metal surfaces have no oxide, whereas in neutral solutions metal surfaces are covered with films of oxides, hydroxides or salts, because the solubility of these species is reduced. Inhibition in neutral solutions is

caused by compounds which can form or stabilise protective surface films. Because of these differences, substances which inhibit corrosion in acid solution by adsorption on oxide-free surfaces, do not generally inhibit corrosion in neutral solution.

Another type of inhibitors in neutral solutions act by stabilising oxide films on the metals to form thin protective, passivating films. Such inhibitors are the anions of weak acids, some of the most important in practice being chromate, nitrite, benzoate, silicate, phosphate and borate. Because of the resistance to the diffusion of metal ions due to passivating oxide films, the anodic reaction of metal dissolution is inhibited; thus these inhibitive anions often are referred to as anodic inhibitors and they are more generally used than cathode inhibitors to inhibit the corrosion of iron, zinc, aluminum, copper and their alloys, in near neutral solutions.

Sheldon, Derby and Van Dem Bussche (17) identified the four major categories of corrosion inhibitors with the mechanism of operation, that is, barrier layer formers, neutralizers, scavengers, and miscellaneous types. The barrier formers were as classified into oxidizers, adsorbed layer formers and conversion layer former. These materials have the ability to deposit on the metal surface and interface with the corrosion reaction and thereby lower its rate to an acceptable value. The neutralizing inhibitors reduce

the corrosivity of the environment by removing hydrogen ions from the environment. Some scavengers operate on a similar principle. Miscellaneous inhibitors include scale inhibitors and biological growths which prevent corrosion by interfering with other processes.

Cohen (18) notes that the inorganic anodic inhibitors for iron usually are either oxidizing anions such as nitrite and chromate, or buffering agents such as borate or phosphate. Oxidizing anions are effective in the presence of oxygen to prevent corrosion, but in general, the effective concentration is lower in the presence of oxygen.

Nitrite ion reacts at the metal surface to form iron oxide and is reducted as far as ammonia $^{(19)}$. The protective film formed on the metal surface is mainly cubic oxide of the $\mathrm{Fe_3O_4}$ - $\mathrm{Fe_2O_3}$ · γ type $^{(20),(21)}$. In the absence of an oxidizing agent, the protective film tends to revert to $\mathrm{Fe_3O_4}$ by reaction with the underlying metal. At a slightly higher potential than the primary passive potential, the protective film breaks down locally in the presence of chloride to form pits, although the film formed reduces corrosion. In the absence of chloride, the film becomes thick with a raising of the potential.

Cohen (22) earlier had found that weight loss decreased as both concentration of nitrite and oxygen increased. At



intermediate concentrations, pitting was observed. During the reaction/exposure of nitrite solution to the specimen, the nitrite ion concentration was found to decrease.

Cohen suggests that a surface film is formed by adsorption of nitrite on the metal surface, followed by a reaction which forms oxide and ammonia. The same adsorption-reaction mechanism was proposed for other oxidizing inhibitors, e.g., chromate and molybdate. Although nonoxidizing inhibitors require the presence of oxygen, a much higher concentration of non-oxidizing oxyanion is required to inhibit corrosion.

Rozenfeld (23), (24) reviewed the effects of nitrite, nitrate and other simple nitrogen-containing compounds for ferrous alloys in both neutral aqueous solutions and in the presence of accelerants, specifically chloride and sulfate ions. The inhibiting properties of sodium nitrite depend on the concentration of accelerant ions in the electrolyte. In solutions containing sodium chloride and sodium sulfate, sodium nitrite accelerates corrosion up to ca. 0.08 g/l concentration, but at higher concentrations, it exerts a strongly inhibitive effect, being maximum at 0.2 g/l concentration (2 wt.%). Rozenfeld suggests that in case of incomplete protection, sodium nitrite diverts a larger part of the surface from the anodic reaction and hence shifts the potential more strongly toward positive values than other inhibitors. The corrosion-intensifying mechanism

involving low concentrations of sodium nitrite is the same as observed for other anodic inhibitors (e.g., chromate and bichromate), i.e., the corrosion rate increases as inhibitor increases up to critical value and then decreases. In the absence of accelerant ions, the protective concentration of sodium nitrite is between 10^{-5} and 10^{-4} mol/l or ca. 6.9 x 10^{-4} wt.%.

The protection concentrations of sodium nitrite are a fuction of the temperature. In the absence of an inhibitor, the corrosion rate of iron increases as the temperature is raised to 50 - 60°C, but at higher temperatures, the corrosion rate decreases because of the lower oxygen solubility. If sodium nitrite is added, but not sufficient to completely suppress the corrosion process, the corrosion rate increases steadily with a rise in temperature. Apparently at high temperatures, the overvoltage for the reduction reaction of sodium nitrite decreases and the inhibitor begins to be reduced at a low rate, hence the limited oxygen solubility can no longer be the factor which restricts the corrosion rate. At high temperature, however, the increase in the concentration of sodium nitrite decreases the corrosion rate. At 25°C, the protective property of steel in distilled water is obtained at 2 x 10^{-4} mole/1, while at 70° C, it is obtained at 5 x 10^{-3} mole/1.

When accelerant ions are present, the logarithm of the protective sodium nitrite concentrations is linear with respect to the concentration of accelerant. The protective properties of nitrite are suppressed most strongly by sulfate ions and less strongly by nitrate ions. Therefore, for the same concentration of accelerant ion, a higher sodium nitrite concentration is needed in the presence of sulfate than in the presence of nitrate for protection. To suppress corrosion in the presence of chloride, a lower sodium nitrite concentration is needed than in the presence of sulfate. As the concentration of accelerant ions increases, the difference between the effects of sulfate and chloride decreases, whereas the difference between chloride and nitrate remains. If high concentrations of the ions are excluded, then, in terms of aggressiveness, accelerants are ordered as follows: sulfate > chloride > nitrate.

In the presence of both accelerant and inhibitive ions, the passivating ion is adsorbed preferentially. Thus, it is harder for nitrite ion to dislodge already-adsorbed chloride ions from the electrode surface than to prevent its initial adsorption. The adsortion of both the passivating ions and the accelerating ions should be facilitated as the potential shifts in the positive direction. Evidently at more positive potentials, the adsortion of chloride is greater than the adsortion of passivating ions, hence the electrode is activated. When various aggressive ions (e.g., chlorides and sulfates) are present, protection is achieved at a sodium nitrite concentration generally greater than

the total concentration of accelerant ions. Corrosion occurs when the ratio of inhibitor concentration to total accelerant-ion concentration is less than one.

Sodium nitrite also is more effective in suppressing the accelerant properties of chloride than are benzoate and chromate. In the presence of sulfate, nitrite is about as effective as chromate. With respect to nitrate, the effectiveness of the different inhibitors decreases in the following order: chromate > benzoate > nitrite. Other compounds containing the NO₂ group and used as corrosion inhibitors include dicyclohexylamine nitrite (DAN) and salts of nitrobenzoic acids (nitrobenzoates). Also according to Rozenfeld and Marshakov⁽²⁵⁾, that concentration of inhibitors required to inhibit crevice corrosion is much higher than for general corrosion.

Marshall⁽²⁶⁾ found that a combination of nitrite with N, N-di-(phosphonomethyl) methylamine was an effective corrosion inhibition for ferrous alloys when compared with nitrite alone. The passive film formed in the presence of a combination of nitrite with N, N-di-(phosphonomethyl) methylamine was more protective and less susceptible to pitting corrosion than the passive film formed in the presence of nitrite alone.

Ledovskikh (27) also has reported that combinations of sodium nitrite with various organic amines inhibit the corrosion of steel in a neutral medium (0.1 M NaCl) and

finds that the protective effect correlates well with physicochemical parameter of the amines (e.g., electron density at the nitrogen atom, ionization constant).

The effect of sodium nitrite in chloride and sulfate media for mild steel has been discussed by Legault and Walker (28). Passivity in these systems resulted from an oxide film and was dependent upon the rate of protective oxide film formation exceeding the rate of the film deterioration. Also, Wachter (29) showed the effectiveness of sodium nitrite under the conditions which obtained in petroleum pipelines. Cohen (30) concluded that the function of nitrite was to maintain the oxide film which was formed by the reaction of dissolved oxygen with the steel surface. Also, it was reported that the sulfate ion interferes with the fuctioning of sodium nitrite as a corrosion inhibitor for mild steel (31).

Mercer, Jenkins and Rhoades-Brown (32) investigated the action of sodium nitrite as a corrosion inhibitor for mild steel in neutral aqueous solution. Surface preparation of mild steel has little effect on the minimum concentration of nitrite required for protection in distilled water. The relationships between nitrite concentration and the maximum concentration of aggressive anion that will permit inhibition is logarithmic. In solutions of low nitrite concentration, the order of anion aggressivity is sulfate >



chloride > nitrate; the order changes with increase in nitrite concentration.

Foley⁽³³⁾ describes the role of chloride in iron corrosion as functioning through its property of penetrating oxide films that otherwise are protective, and adsorption on the metal surface or the thin oxide film to produce a strong electric field which draws ions from the metal⁽³⁴⁾. The halide ion forms a surface complex with Fe, the stability of which determines the corrosion kinetics and catalyzes the reaction by forming some sort of intermediate bridging structure.

Corrosion rates of iron in chromate and nitrite solutions were measured as weight loss by Matsuda and Uhlig⁽³⁵⁾. The critical concentration below which corrosion increases or pitting occurs is 1×10^{-5} M for NaNO₂ and 5×10^{-4} M for Na₂CrO₄. In the presence of Cl⁻ and SO₄²⁻, these values are increased. Sulfates break down passivity in nitrite solutions more than chlorides do, the reverse is true in chromate solution.

Oxyanions of various elements (e.g., chromium and molybdenum) are corrosion inhibitors for ferrous alloys in neutral aqueous solutions. In acid solutions, these oxidants become cathodic depolarizers and they influence the anodic reaction of iron, as discussed by Mikhailovskii,



Popova and Sokolva⁽³⁶⁾. Inhibiting properties are attributed either to a capacity to "repair" the oxide film formed on the metal in an electrolyte or to adsorption of the oxyanion, resulting in a change in structure of the metal-electrolyte boundary. The influence of oxidizing agents usually is attributed to their enhanced adsorption capacity favoring formation of surface complexes which retard the anodic ionization of the metal.

McCafferty (37) classes inhibitors as (a) adsorption (chemisorption), (b) film-forming/passivating, and (c) precipitation. Crevice corrosion of iron accelerated by chloride and inhibited by chromate has been discussed further by McCafferty (38), finding that the process can be inhibited successfully at chloride concentrations up to 0.6 M/1 (3.5 wt.%). The logarithms of each ion's activities are linearly related at the minimum chromate activity neccessary to inhibit crevice corrosion. McCafferty explained this on the basis of competitive adsorption between the aggressive and inhibitive ions, each of which adsorbs. Steady-state electrode potentials of crevice-corroding iron were found to be - 620 to - 660 mV vs. Ag/AgCl reference electrode, and independent of bulk solution composition.

Samuel, Sotoudeh and Foley (39) proposed steps by which aggressive anions act on aluminum:



- Adsorption of Cl on aluminum oxide (Al₂O₃) surface.
- 2. Complexing of aluminum cation (Al⁺³) in the oxide lattice with halide ion (e.g., Cl⁻) to form soluble AlCl₄⁻.
- 3. Soluble species (AlCl₄⁻) diffuse away from the surface resulting in a thinning of the protective oxide film.
- 4. At sufficiently thinned sites aluminum reacts directly with the electrolyte.

Soluble species diffuse away from the reaction site and the oxide film is thinned to a point where aluminum ions can pass directly from the metal to the solution interface.

The critical step then is the formation of soluble complexes at specific sites. For this reason pitting and general corrosion of aluminum depend on the nature of the anion. The preferential adsorption sites may be defects or flaws in the oxide film.

An inhibitor may participate in either of the first two steps:

- Competing for adsorption sites, hence retarding formation of soluble species.



- Competing in the reaction Al⁺³ + 4Cl⁻ = AlCl₄⁻
to prevent formation of AlCl₄⁻; hence the competing ion must form an insoluble complex.

In chloride solution, the passivity of inhibition should be viewed as interfering with the reaction

$$Al^{3+} + 2Cl^{-} + 2OH^{-} = Al(OH)^{2}Cl_{2}^{-}$$

whereby the oxide film is thinned. A species may form a complex ion which may be stable and soluble

$$Al^{3+} + nR^{-} = AlR^{3-n},$$

and accelerate corrosion. On the other hand, the species may react as

$$Al^{3+} + 3R^{-} = AlR_{3},$$

wherein the species ${\rm AlR}_3$ is stable, unshared, very slightly ionized, and resides at or near the aluminum surface.

Vedder and Vermilyea $^{(40)}$, $^{(41)}$ showed the relation between aluminum and water mechanism which involves formation of amorphous ${\rm Al}_2{\rm O}_3$, dissolution of the ${\rm Al}_2{\rm O}_3$, and precipitation of AlooH from solution. The AlooH layer

provides deposition sites near the surface for dissolved species hence allows the reaction to proceed at a high rate despite the very low solubility of ${\rm Al}_2{\rm O}_3$ in neutral solutions. Inorganic inhibitors function by becoming adsorbed on the oxide and preventing the nucleation and growth of the hydroxide layer $^{(41)}$.

The adsorption of ³⁶Cl on an aluminum surface was found to be a function of time and applied voltage, and highly localized to oxide imperfections and grain boundaries, as discussed by Verkerk⁽⁴²⁾. Belov and coworkers⁽⁴³⁾ established the following order for the degree of adsorption onto an anodic aluminum film:

$$H_2O < NO_3^- < Cl^- < Cr_2O_4^{2-} < SO_4^{2-} < H_2PO_4^-$$

A similar order also was reported by Herczynska and Prozynska $^{(44)}$ for NO $_3^-$, Cl $^-$ and SO $_4^{2-}$. Berzins, Lowson and Mirams $^{(45)}$ measured the adsorption isotherms for chloride on a corroding aluminum surface using 36 Cl as a radioactive tracer. The amount of chloride adsorbed, W_{Cl} was a function of chloride concentration, [Cl $^-$], and time, t, according to;

$$log W_{Cl} = 0.64(log[Cl^-] + log t) - 78,$$

where W_{Cl} was expressed as g cm⁻², [Cl] as mol l⁻¹ and t as minutes. The adsortion was localized to corroding pit sites and there was no threshold for the chloride concentration below which pitting would never occur and the addition of inhibitor (e.g., nitrate or sulfate) would delay but not prevent the onset of pitting. The delay time before the onset of pitting varied a logarithmically with inhibition concentration according to

$$log D = 1.4 log C_1 + K_1$$

where \mathbf{K}_1 was constant and was a function of chloride concentration and inhibitor species, D as delay time and \mathbf{C}_1 as inhibitor concentration.

Foroulis and Thubrikar (46) investigated the kinetics of passivity breakdown and nucleation of pitting of preanodized aluminum by chloride. The rate of passivity breakdown at steady-state, critical pitting potential was dependent on chloride concentration, temperature, and oxide film thickness, but is independent of solution pH in the range 5 - 10. It is likely that in the process of pit initiation, adsorption of chloride from solution on the hydrated aluminum oxide surface is the rate-determining step in low chloride concentration, whereas the reaction step resulting in formation and dissolution of the hydroxylchloride aluminum salt on the hydrated oxide surface becomes the rate-determining step in higher chloride concentration.



The influence of anions on the initiation of pitting and the kinetics of pit growth on aluminum alloy Type 7075 has been investigated by Dallek and Foley⁽⁴⁷⁾. The order of reaction (i.e., the number of aggressive anions per Al surface reaction site) and the energy of activation for pitting initiation in aggressive anion-containing solution were measured. The value of the order of reaction (n) and the activation energy (E_a) in 1 N H_2SO_4 varies with the aggressive anions as n = 8, E_a = 18 kcal mole⁻¹ for Cl⁻, n = 4, E_a = 26 kcal mole⁻¹ for Br⁻ and n = 2, E_a = 6.6 kcal mole⁻¹ for I⁻.

Nguyen and Foley (48) investigated the dissolution reaction at a bare aluminum surface in aqueous solutions and concluded that the controlling step was a complexation reaction of hydrated cation with the aggressive anion present, which accounted for the strong anion dependence in metal pitting and general corrosion, although hydrolysis of complexes lead to the formation of stable hydrous oxides whose composition was independent of the anion in solution.

Samuel, Sotoudeh and Foley⁽³⁹⁾ also have reported that a chelate, an ion or molecule with two or more atoms having unshared pairs of electrons, might inhibit corrosion or accelerate corrosion. The hydroxy carboxylic acids form soluble chelate compounds with aluminum and corrosion in



chloride solution is increased by an order of magnitude. Carboxylic acids form stable compounds which function in the same manner as do precipitating inhibitors, although the behavior of either may depend on the concentration of the coordinating compound.

The role of complex ions in the corrosion reaction with potential energy has been clarified by Foley and Nguyen (49). Generally speaking, one or more complex ions are involved in a multistep sequence. The relative stability of the complex is the critical factor. The formation of an uncharged, stable, basic salt in a deep energy valley will prevent the reaction from progressing along the reaction coordinate, which was illustrated by comparison of the Cl and SO₄ systems. In both cases, initial formation of the complex species was quite rapid, but the sulfate species lay at a low energy level resisting forward movement along the reaction coordinate. Thus chloride was aggressive, but sulfate was not in all corrosion reactions such as pitting and stress corrosion.

Locking and Mayne (50) investigated the corrosion of aluminum at room temperature in solutions over pH range 2.0 - 12.0 and found that corrosion was dependent more on the nature of the anion than on the pH of the solution.



Bohni and Uhlig⁽⁵¹⁾ investigated the environmental factors affecting the critical pitting potential of pure aluminum, - 0.40 V (SHE). This value was not greatly sensitive to temperature (0 - 40°C), to small alloying additions of Mn or Mg, nor to thickness of oxide film produced by anodizing, which was more active in the high Cl⁻ concentration, but became more noble with additions to NaCl of nitrates, chromates, acetates, benzonates or sulfates which were effective as pitting inhibitors in increasing order. The pitting is relative to competitive adsortion on Cl⁻ with oxygen for sites on the metal surfaces. Inhibitors competed in turn with Cl⁻ ions, making it necessary to shift the potential in the positive direction in order for Cl⁻ to adsorb followed by pit initiation.

On the other hand, for 18-8 stainless steel, increasing Cl concentration shifts the critical potential to more active values as discussed by Leckie and Uhlig (52). The potential is shifted to more noble values by the presence of other anions, e.g., ${\rm Clo}_4^-$, ${\rm So}_4^{2-}$, ${\rm NO}_3^-$, ${\rm OH}^-$, at sufficient concentrations of which act as pitting inhibitors. Lowering the temperature produces a similar effect of enobling the critical potential.

It was known that borax-nitrite formulations were effective inhibitors for aqueous corrosion of iron, steel,



and aluminum alloys $^{(53)}$. It was reported that formulations such as molybdate-nitrite $^{(54)}$, $^{(55)}$ and benzoate-nitrite $^{(56)}$, $^{(57)}$ also provided effective inhibition for these alloys in tap water.

Khobaib, Quakenbush and Lynch (59) have studied corrosion inhibition effects of nitrite-borax mixtures (as well as other combinations) on both ferrous and aluminum alloys. These were found to be effective in both distilled water and tap water, but in chloride concentrations comparable with sea water, they were ineffective at low concentrations. Certain surfactants, however, significantly enhanced corrosion inhibition in water of high chloride concentration.

In a further study, Khobaib⁽⁵⁹⁾ evaluated the inhibiting efficacy of more than 200 formulations of organic and inorganic compounds in the presence of urine for use as airplane bilge inhibitors. The most effective combinations again involved borax, sodium nitrite and a variety of surfactants. These formulations were developed by systematic exploration of compositions suggested by Green and Boies⁽⁶⁰⁾.

Nguyen and Foley⁽⁶¹⁾ implied that the corrosive or non-corrosive state of a metal in a given environment depended on the stability of the complex species formed on the film and on the affinity of the anion present, that is,

support the first step among steps established by Samuel et al⁽³⁹⁾, to react with the exposed metal. Nitrate ion was reduced to ammonia by elementary aluminum but not by alumina.

Mckissick, Adam and Foley⁽⁶²⁾ reported that in specific electrolyte mixtures, i.e., specific concentrations and specific NaCl - NaNO₃ ratios, the corrosion of aluminum alloy Types 7075 and 2024 was increased by an order of maginitude over that in NaCl solutions of the same concentration.

Anderson and Hocking (63) had examined the behavior of aluminum during anodic polarization in electrolytes containing anodic inhibitors (e.g., CrO_4^{2-}) and chloride ion. They had established the existence of a critical potential of film breakdown above which pitting corrosion occurred. This potential was dependent upon electrolyte composition, which meant that competitive adsorption of anions at the film-solution interface determined the anodic reaction.

In summary, it is suggested that a variety of physicochemical properties of accelerant/inhibitors may be involved in the corrosion process. Many published studies contain hints as to which properties may be critical, e.g., ionic charge, size, mobility, ionization state, adsorption, etc., but systematic exploration of accelerant/inhibitor



chemistry is needed for elucidating the crucial properties in corrosion. The nitrogen system, consisting of the oxyanions and ammonium ion, presents an excellent system for systematic evaluation of these factor.

D. The Oxyanions of Nitrogen

The oxyanions of nitrogen are listed in Table 1 together with apparent oxidation state. Although all of them can form free acids, only nitric acid can be considered stable in aqueous solution or as the pure acid; all the rest decompose with varying degrees of violence. All can be prepared as relatively stable salts, particularly the sodium salt, although the preparations of the salts themselves are somewhat hazardous. The oxidation/reduction and inhibitive properties of these ions are related to their stability characteristics.

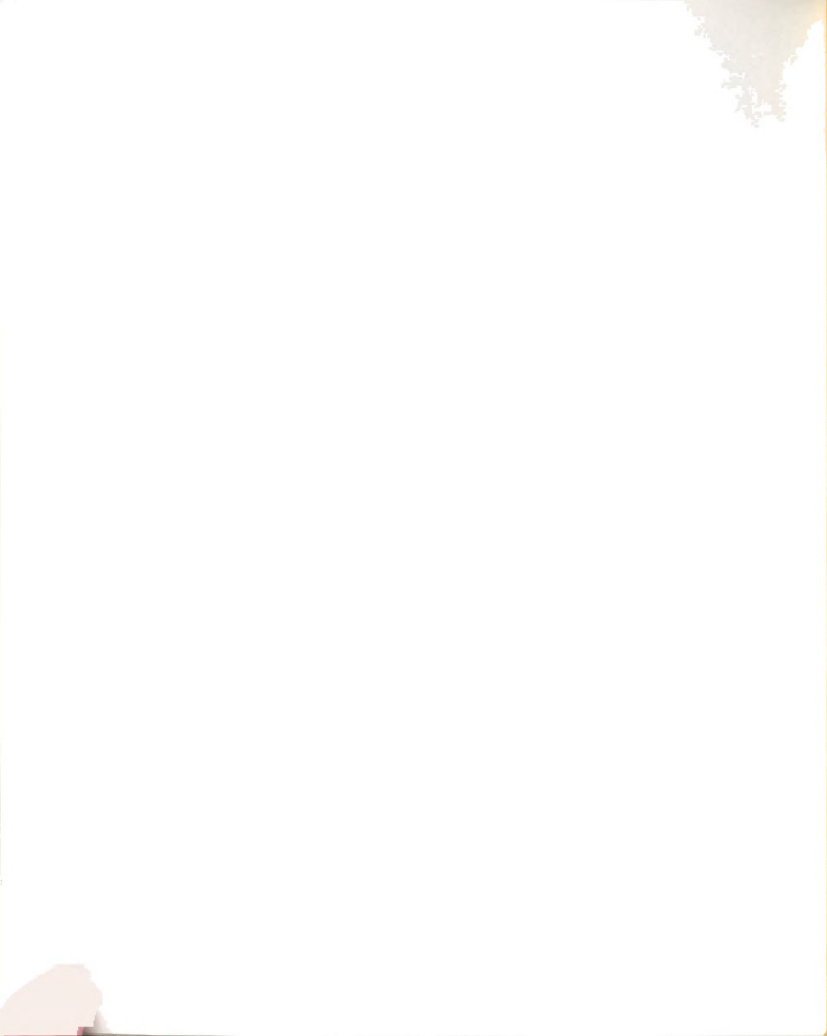
1) Nitrite

Sodium nitrite is a readily available laboratory reagent. Nitrous acid and the nitrites are most commonly employed as oxidizing agents, although strong oxidants (e.g., electric current, MnO₂, and Cl₂) convert nitrous to nitric acid in alkaline solution.



Table 1. The Oxyanions of Nitrogen (64)

Formula	Name	Apparent	Oxidation	State	of N
NH ₄ ⁺¹	ammonium		-3		
N ₂ O ₂ ⁻²	hyponitrite		+1		
N ₂ O ₃ ⁻²	nitrohydroxylama	te	+2		
NO ₂ ⁻²	hydronitrite		+2		
NO ₂ ⁻¹	nitrite		+3		
NO ₃ -1	nitrate		+5		
NO ₄ -1	peroxynitrate		+5		



Structurally, the nitrite ion belongs to the point group C_{2v} which is not linear, but bent. Two resonance structures are postulated (Figure 3). The ONO bond angle is consistent with sp^2 hybridization at the nitrogen atom, but the N-O bond lengths are closer to a bond order of 2 than 1.5.

Important couples describing that nitrites are employed as oxidizing agents are

$$N_2O + 3H_2O = 2HNO_2 + 4H^+ + 4e^ E_{298}^O = -1.29 \text{ volts}$$
 $NO + H_2O = HNO_2 + e^ = -0.99 \text{ volt}$
 $HNO_2 + H_2O = NO_3^- + 3H^+ + 2e^ = -0.94 \text{ volt}$

in acidic solutions, and

$$N_2O + 6OH^- = 2NO_2^- + 3H_2O + 4e^ E_{298}^O = -0.15 \text{ volt}$$
 $NO + 2OH^- = NO_2^- + H_2O + e^-$ = 0.46 volt
 $NO_2^- + 2OH^- = NO_3^- + H_2O + 2e^-$ = -0.01 volt





Figure 3. Electronic Structure of NO_2^{-1} .



in alkaline solutions. The potential in acidic solutions is positively greater than that in alkaline solutions, and the free energy for reduction in the acidic solutions is smaller than in the alkaline solutions. Thus the greater oxidizing strength in acidic solutions is apparent.

2) Nitrate

Sodium nitrate is readily available. In general, the nitrate ion is planar (D_{3h} symmetry) with all N-O bond distances close to 1.22Å. This can be represented in valence bond terms by resonance structures based on those illustrated by Figure 4. Molecular orbitals also can be constructed for the nitrate ion on the basis of three bonds using sp² hybrid orbitals, the p₂ orbitals of nitrogen, and three oxygens combining to form a π orbital containing two electrons.

The data in the Table 2 show the wide variety of reduction reactions available and their relations to other nitrogen oxyanions and compounds. Also shown are stepwise reduction processes of nitrogen (V) to nitrogen (III). As with the case of nitrite, comparing the magnitude of potentials and driving force, the effect of acid media on the oxidizing power of nitrate is clearly evident.

3) Hyponitrite

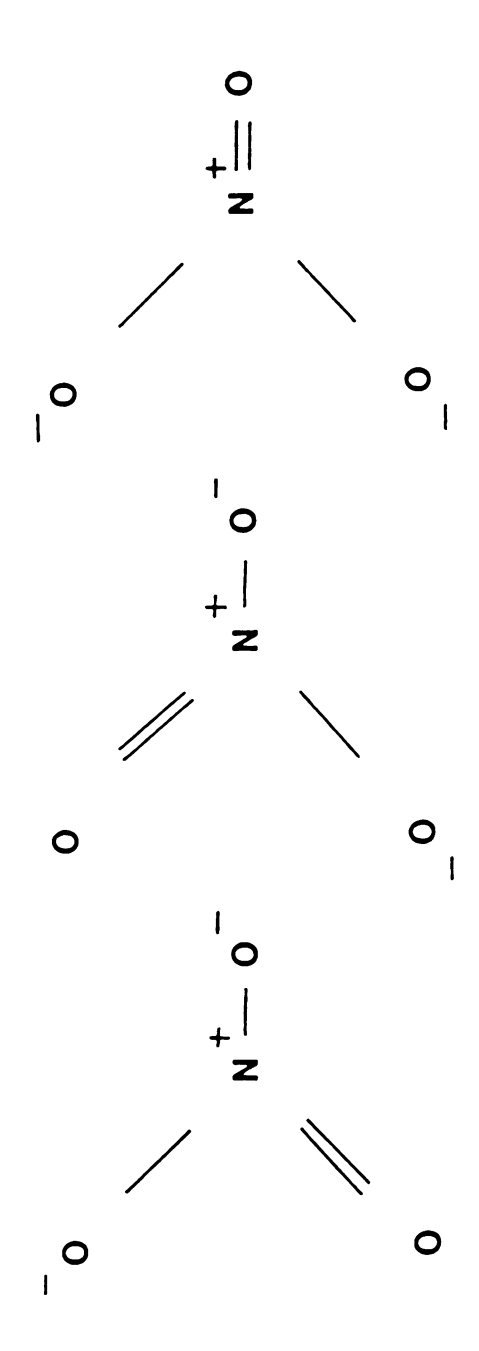


Figure 4. Electronic Structure of NO₃-.

Table 2. Oxidation Potential Data for Reduction of Nitrate Ion (65)

Alkaline Solutions	$\begin{array}{llllllllllllllllllllllllllllllllllll$	
Acidic Solutions	88e 8e	



Hyponitrite is known chiefly in the form of its salts, although free hyponitrite acid, $H_2N_2O_2$ can be prepared as white deliquescent plates; however, it is explosively unstable. Aqueous solutions of the acid are relatively stable: At pH 1 - 3 and 25°C, the acid has a half-life of 16 days, but at pH 4 - 14, it is quite stable. The acid ionizes as a weak dibasic acid,

$$k_{1} k_{2}$$

$$H_{2}N_{2}O_{2} = H^{+} + HN_{2}O_{2}^{-} = 2H^{+} + N_{2}O_{2}^{2-}$$
where,
$$k_{1} = 9 \times 10^{-8} \text{ and } k_{2} = 1 \times 10^{-11} \text{ at } 25^{\circ}\text{C}$$

It is reported that the first and second heats of ionization for hyponitrous acid are 3.7 and 6.1 kcal/mol⁽⁶⁷⁾, respectively, the sum of which equals 9.8 kcal/mol, a value lower than that obtained calorimetrically by Latimer and Zimmerman (11.1 kcal/mol)⁽⁶⁸⁾. The enthalphy of formation of aqueous $HN_2O_2^-$ and $H_2N_2O_2$ is -12.4 and -15.4 kcal/mol respectively⁽⁶⁹⁾. In higher pH solution, the hydrogen hyponitrite ion is unstable,

$$HN_2O_2 = N_2O + OH$$
.

Thus, the characteristics of the hyponitrite ion related to corrosion can be examined readily, particularly in mild acid to alkaline solutions.

The strong absorption $^{(70)}$ in the ultraviolet region at 248 m μ (ϵ =3980) is characteristic of compounds containing the N=N bond, which suggests that the bonding in the hyponitrite ion is adequately described by Figure 5 with trans or cis configuration. It has been shown by Raman $^{(72)}$, $^{(73)}$ and infrared studies $^{(74)}$, $^{(75)}$ that the product obtained in the usual preparative reactions is the trans isomer. Such a planar trans centrosymmetric structure belongs to the C_{2h} point group.

The hyponitrite metal salts are prepared generally by reduction of the nitrate ion, commonly by sodium amalgam,

$$2NaNO_3 + 8Na/Hg + 4H_2O ----> Na_2N_2O_2 + 8NaOH + 8Hg.$$

Sodium hyponitrite decomposes on heating to 260° C in vacuo or 335° C at atmospheric pressure to give sodium oxide, nitrite and nitrate together with nitrogen. It is partially hydrolyzed in water or dilute acids to N₂O, NO₄, and N₂ but it is oxidized by permanganate. Hyponitrites possess both reducing and oxidizing properties as indicated by the couples



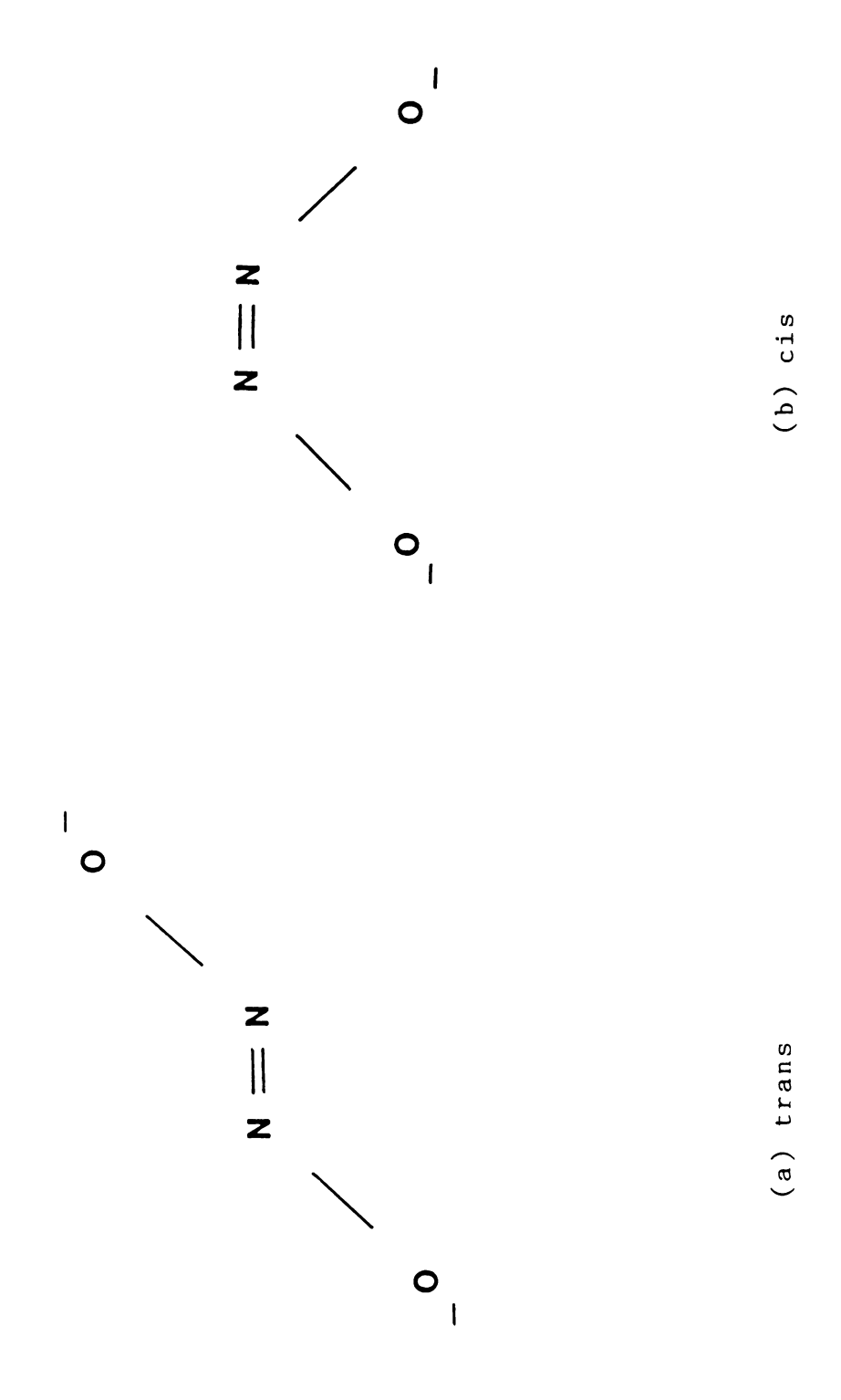


Figure 5. Electronic Structure of $N_2O_2^{2}$.



$$H_2N_2O_2 = 2NO + 2H^+ + 2e^ E_{298}^O = -0.712 \text{ volt}$$
 $H_2N_2O_2 + 2H_2O = 2HNO_2 + 4H^+ + 4e^ = -0.86 \text{ volts}$ $N_2 + 2H_2O = H_2N_2O_2 + 2H^+ + 2e^ = -2.75 \text{ volts}$ $2NH_3OH^+ = H_2N_2O_2 + 6H^+ + 4e^ = -0.44 \text{ volts}$

in acidic solution, and the couples

$$N_2O_2^{-2} = 2NO + 2e^ E_{298}^0 = -0.10 \text{ volt}$$
 $N_2O_2^{-2} + 4OH^- = 2NO_2 + 2H_2O + 4e^ = 0.18 \text{ volt}$
 $N_2 + 4OH^- = N_2O_2^{-2} + 2H_2O + 2e^ = -1.60 \text{ volts}$
 $2NH_2OH + 6OH^- = 5N_2O_2^{-2} + 6H_2O + 4e^ = 0.73 \text{ volt}$

in alkaline solution. However, the reducing properties predominate. Strong oxidizing agents will convert hyponitrites to nitrates.

d) Ammonium Hydroxide

The extent to which aqueous ammonia exists as $\mathrm{NH_4OH}$ or as hydrated $\mathrm{NH_3}$ has long been discussed $^{(76)}$. Ammonium ion is very soluble in water in which it is involved in the equilibrium

$$NH_3 + H_2O = NH_4^+ + OH^-$$

$$[NH_4^+] [OH^-]$$

$$K = ----- = 1.65 \times 10^{-5} \text{ at } 25^{\circ}C.$$

$$[NH_3]$$

Solution of ammonia react with acids, taking up protons to form ammonium ions

For this reason, ammonium solutions give only a weakly basic reaction or, alternatively, behave like solutions of weak base. The equilibrium is displaced strongly to the left because of the extremely slight dissociation of water. There are, accordingly, only a few ammonium ions present in an aqueous solution of ammonium and correspondingly few hydroxyl ions.



E. Research Program

The object of this research program was an experimental exploration of the relations between accelerant/inhibitor properties and the electrochemistry and electrokinectics of corrosion in aluminum. A variety of inhibitor/accelerants were under study. These included (a) ordinary reagent-grade chemicals, e.g., NaCl, NaNO₂, NaNO₃, and NH₄OH, (b) the Lynch formulation mentioned in Section III-C and Na₂B₄O₇, and (c) other compounds of nitrogen, specially sodium hyponitrite (Na₂N₂O₂).

A potentiodynamic polarization technique was used to investigate the effectiveness of inhibitor when a 7075 - T6 high-strength aluminum was exposed to solutions with and without chloride ions.



III. Experimental Test Procedure And Apparatus

Many corrosion phenomena can be explained in terms of electrochemical reactions, hence electrochemical techniques can be used to study these phenomena. Measurements of current-potential relations under controlled conditions can yield information on corrosion rates, coating and films, passivity, pitting tendencies and other important data.

Potentiodynamic anodic polarization is the characterization of a metal specimen by its current-potential relationship. This is fast and reproducible, and clearly indicates the open circuit potential, the corrosion current density in the passive range and pitting potential. The specimen potential is scanned slowly in the positive- or negative- direction. These measurements are used to determine corrosion characteristics of metal specimens in aqueous environments. A complete current-potential plot of a specimen can be measured.

A. Experimental System

The experimental system consisted of:

- (1) Potentiostat and Logarithmic Current Converter
- (2) Waveform Generator and Recorder
- (3) Corrosion Cell
- (4) Electrometer Probe



(5) Heat Source

The experimental arrangement used in this study is shown in Figure 6.

(1) Potentiostat and Logarithmic Current Converter

The potentiostat was a Princeton Applied Research (PAR) Model 173, an electrochemical measuring instrument. Operated as a potentiostat, the potential between electrodes of an electrochemical cell is held constant; operated as a galvanostat, the current through a cell is held constant.

The instrument featured a current capability of one ampere with compliance voltage as high as 100 V in either polarity and a slew rate of 10 V per microsecond. It incorporated two independent built-in potential/current sources, each adjustable to any voltage in range of ±4.999V as well as logic and switching circuity for controlling the sources from the front panel or by externally derived triggers. Two additional external potential/current programming signals might be added to those provided by the instrument, and a wide variety of triggering and switching waveforms might be employed to control the applied potential/current programs.

The logarithmic current converter was an EG & G PAR Model 376. The Model 376 was ideally suited to use in those applications where the current varied over many orders of



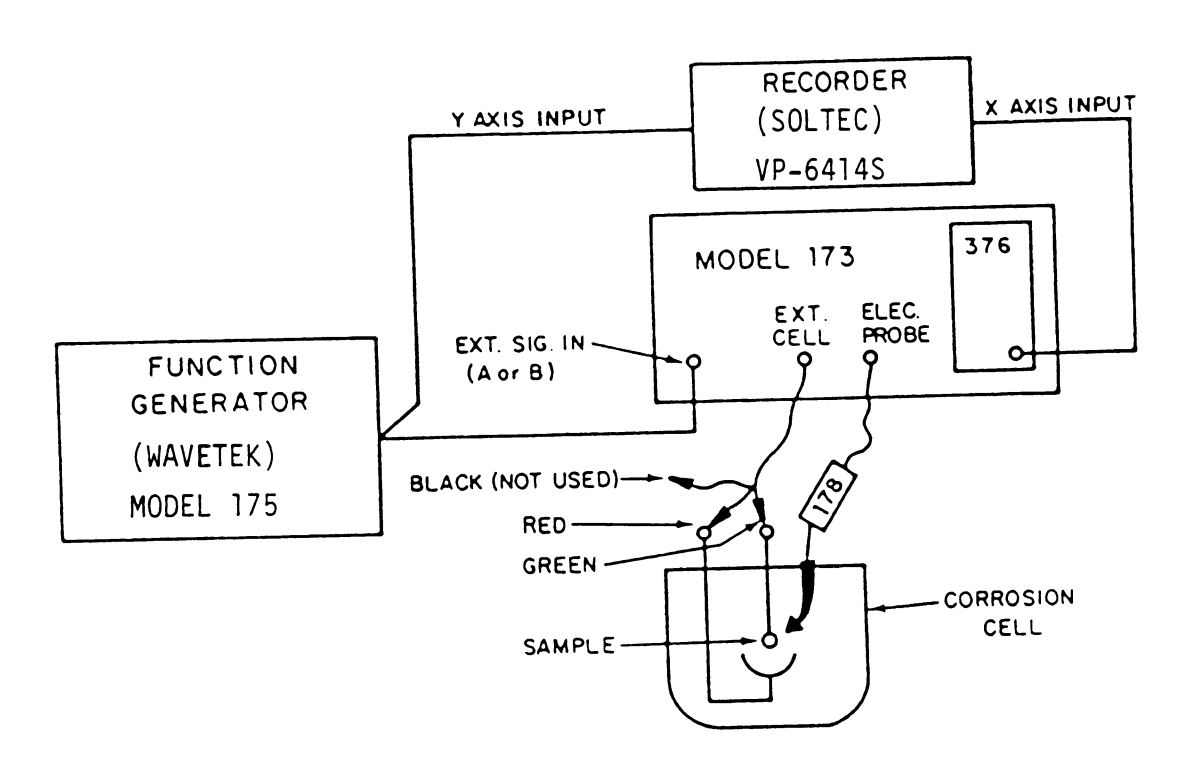


Figure 6. The Experimental System.



magnitude in the course of the experiment. Like the Model 176, the Model 376 provided an output voltage proportional to the cell current. However, it additionally provided an output voltage proportional to the log of the cell current. There was provision for displaying the current of the log of the current on the Model 173 panel meter. In displaying the current, full-scale meter deflection indicated a current of 1, 2, or 5 times the selected Current Range, the same as for the Model 176. In the Log Meter mode, full-scale deflection indicated a current 1, 2, or 5 decades below the selected current range.

(2) Waveform Generator and Recorder

Waveform generator used was Wavetek Model 175. The Model 175, Arbtrary Waveform Generator generates any waveform that can be expressed as a function of time. The working Random Access Memory (RAM) had four sets of 256 addresses and each address accepted an 8 bit word. This corresponded to a 1024 (time) by 255 (amplitude) matrix in which to draw waveforms. These storage addressess can be loaded manually by front panel controls or remotely loaded via the GPIB interface. There are four fixed waveforms: sine, square, triangle and ramp. In this study, the ramp waveform was used.

The recorder used was Soltec VP-6414S X-Y Recorder. This recorded a relation of the form f(x) = y between two



variables on A 4 chart paper. The range was from 2 mV/cm to 1 V/cm.

(3) Corrosion Cell

The Model K47 Corrosion Cell System of PAR was used in this study. Figure 7 shows a corrosion cell for polarization measurements.

(a) Working Electrode

The working electrode for this investigation was a square shaped specimen with surface area of one \mbox{cm}^2 .

(b) Reference Electrode

A saturated calomel electrode (SCE) was used as the reference electrode. The SCE is not easily poisoned or contaminated and is insensitive to electrolyte composition because of its design. A solution bridge from the Luggin capillary to another beaker containing the reference electrode made the electrical connection between this electrode and the solution. This liquid junction was used to avoid the contamination of the solution. The SCE incorporated an unfired Vycor^R tip designed specially to provide ultra-low liquid leakage rates and minimum IR drop through the tip. This arrangement eliminated complication arising from poisoning of test solutions by filling solutions, and allowed high sensitivity operation of potentiostat and



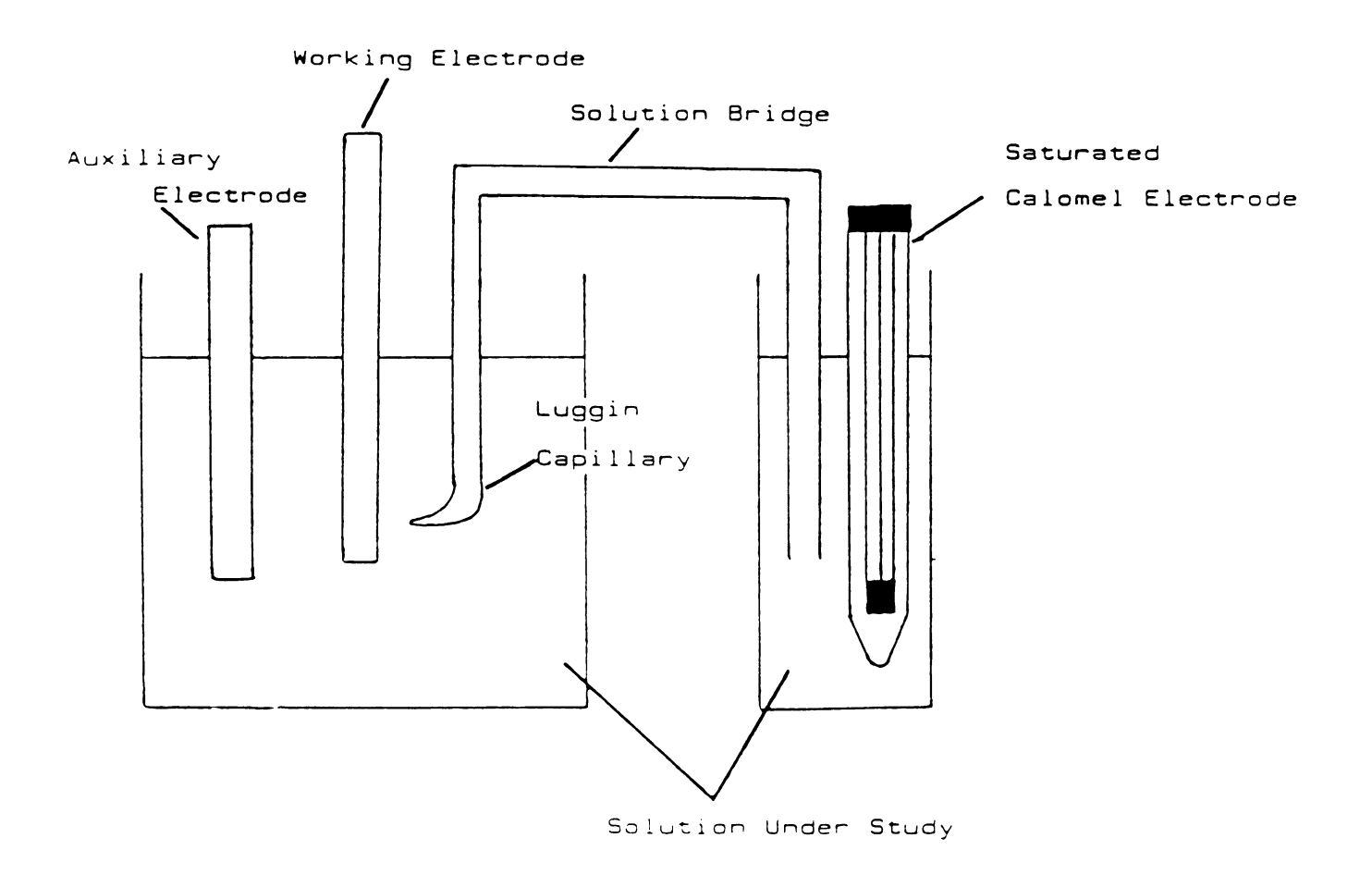


Figure 7. The Corrosion Cell.



polarographic analyzers. Vycor^R is a semipermeable membrane which filters out particles smaller than virus. The average pore diameter was 4 millimicrons, and the apparent density in a dry state was 1.45 nm.

(c) Auxiliary Electrode

A couple of the high density graphite was employed as the auxiliary electrode to transfer current to or from the working electrode.

(4) Electrometer Probe

A PAR Model 178 Electrometer Probe was used in Controlled Potential operation to monitor the reference Electrode, and could be used at any time to monitor some potential of interest. The Electrometer Probe was placed at the end of a cable so as to allow the electrometer circuity to be positioned as close as possible to the monitored point, and thereby achieve minimum loading of high impedance electrodes and optimum loop stability in closed loop operation.

(5) <u>Heat source</u>

Since the temperature of the solution was investigated, a heating source was needed. A water bath and the hot plate were used to heat the solution. The solution was

maintained during the test at 0° C, room temperature, 50° C, 75° C, 90° C, $\pm 2^{\circ}$ C.

B. Experimental Technique

Model K47 Corrosion Cell System of PAR was used for the electrochemical measurements of corrosion phenomena which required a cell system that was versatile, convenient to use, and that could provide reproducible conditions from one experiment to another so that a rational comparison between specimens and/or environments could be drawn.

Step 1; Initial stage

- a) The cell was washed and rinsed throughly with distilled water and acetone, and finally rinsed with the electrolyte used. 1 L solution (electrolyte) was made by dilution of high concentration solution and poured into the cell to cover the entire surface of the specimen under test.
- b) The reference, working electrode and reference electrode bridge tube were also washed and rinsed with distilled water, acetone and the electrolyte to be used. The bridge tube was filled with the electrolyte used in the flask. The reference electrode was inserted into the bridge tube, making sure that the bottom of the electrode contacted the solution in the bridge tube. The bridge tube was adjusted

so that the $Vycor^R$ tip was positioned to within about 2 mm of the specimen surface.

Step 2; Equilibration

When a metal specimen was immersed in an electrolyte, both reduction and oxidation processes occurred on its surface. Typically, the specimen oxidized (corroded) and the electrolyte was reduced.

When the specimen was in contact with the electrolyte, the open circuit corrosion potential, E_{CORR} was measured as a function of time in order to find the time to equilibrium. A specimen at E_{CORR} had both anodic and cathodic currents present on its surface. However, when there was no net current to be measured, the specimen was at equilibrium with the electrolyte. E_{CORR} could be defined as the potential at which the rate of oxidation was exactly equal to the rate of reduction. The time to equilibrium was variously depending on the electrolyte. Without sodium chloride, the potential reached a constant value within 3 hours, but with sodium chloride, more than 3 hours for equilibrium was needed. During this time, the electrode was electrically disconnected from the potentiostat.

Step 3; Operation



After reaching equilibrium, the equipment was set up and connected to the system as shown in Figure 1. Whenever the potentiostat was connected to the cell, the potential of the working electrode vs. the reference electrode was displayed automatically on the Model 258 Digital Multimeter. In order to measure the corrosion potential, the Cell Select switch of potentiostat was set to Ext. CELL with Direct Operating Mode. Then corrosion potential was displayed on the multimeter which was connected to the output of the potentiostat.

After the corrosion potential was measured, the Waveform Generator was programmed so that the scan rate of potential was 10 mV/min from the corrosion potential through + 1.5 V for anodic polarization and - 1.5 V for cathodic polarization vs. SCE. If the specimen was polarized slightly more positive than $E_{\rm CORR}$, then the anodic current predominated at the expense of the cathodic current. As the specimen potential was driven further positive, the cathodic current component became negligible with respect to the anodic component. Obviously if the specimen was polarized in the negative direction, the cathodic current predominated and anodic component became negligible.

Control E operation of the potentiostat was always used. When ready to start, the Selector switch was set to Ext. CELL and Ext. SIG INPUT was turned on after programming the Waveform Generator. The counter electrode was driven to whatever the potential was required to establish



the working electrode. The polarization characteristics were obtained by plotting the current response as a function of the applied potential. Since the measured current varied over several orders of magnitude, the log current function was plotted versus potential on a semi-log chart.

C. Alloy 7075-T6 Handling, Cleaning, and Test Solution

(1) Specimen

Commercial aviation-grade 7075-T6 aluminum alloy was used for this study. Tables 3 and 4 show the nominal chemical composition and the mechanical properties of 7075-T6 Al alloys.

(2) Specimen Preparation

a) Polarization Test

7075-T6 Al alloy was cut with the surface area of one cm² to the nearest of 0.01 cm which was measured by using the vernier calipers. The specimen was mounted with copper wire for electrical conduction. The specimen was prepared within one hour of the experiment by wet-grinding and wet-polishing with 240-grit SiC paper to 600-grit SiC paper until previous course scratches were removed. The sample was cleaned thoroughly with distilled water and acetone.



Table 3. Chemical Composition (79)

7075-T6 Al Alloy

Element	Zn	Mg	Cu	Cr	Si	Al	
Wt.%	5.98	2.51	1.67	0.18	0.12	Bal.	

Table 4. Mechanical Properties of 7075-T6 Al Alloy

	ile Strength ksi)	Yield Strength (ksi)	Elongation (%)
Specimen (79)	84.3	74.6	12.0
Handbook ⁽⁸⁰⁾	83.0	73.0	11.0

b) Test Solution

i) Solutions studied

Each specimen was tested in a series of solutions of various concentration of inhibitors with and without sodium chloride. The test solutions are listed in Table 5. Table 6 shows the Lynch Formulation.

ii) Solution Preparation

Each solution was obtained by dilution of a 10 wt. $^{\circ}$ solution except Na $_2$ B $_4$ O $_7$ (1 wt. $^{\circ}$) and Na $_2$ N $_2$ O $_2$. In the case of NH $_4$ OH, the 10 wt. $^{\circ}$ concentration was made using the volume and density of the fresh ammonium hydroxide. Concentrations were expressed on a weight percentage basis. All tests were conducted in unstirred solutions.

iii) Preparation for Sodium Amalgam (79) and Sodium Hyponitrite (80)

iii-1) Sodium amalgam

The Fieser procedure (81) gave especially pure material: A clean sodium piece (6.9 g for an amalgam containing 2% Na, 10g for one containing 3% Na) was placed in a 250 ml three-neck round-bottom flask. The two side necks carried nitrogen inlet and outlet tubes, while the center

Table 5. The Test Solutions

Solutions	Concentrations(wt.%)			
Distilled Water				
NaCl	0.1			
NaNO ₂	0.05, 0.1, 0.5, 1.0, 3.0			
NaNo ₂ + NaCl	(0.05,0.1), (0.1,0.1), (0.5,0.1)			
	(1.0,0.1), (8.0,0.1)			
$NaNO_2 + Na_2B_4O_7$	(0.1,0.1), (0.1,0.5), (0.1,3.0)			
$NaNO_2 + Na_2B_4O_7 + NaC1$	(0.1,0.1,0.1), (0.1,0.5,0.1)			
	(2.0,2.0,0.1), (3.0,3.0,3.0)			
Lynch Formulation (52)	0.513			
Lynch Formulation + NaCl	(0.513,0.1), (0.513,3.5)			
NaNO ₃	0.05, 0.1, 0.5, 1.0,			
NaNO ₃ + NaCl	(0.05,0.1), (0.1,0.1), (0.5,0.1)			
	(1.0,0.1),			
Na ₂ N ₂ O ₂	0.05, 0.1, 0.5			
Na ₂ N ₂ O ₂ + NaCl	(0.05,0.1), (0.1,0.1), (0.5,0.1)			
NH ₄ OH	0.05, 0.1, 0.5, 1.0			
NH ₄ OH + NaCl	(0.05,0.1), (0.1,0.1), (0.5,0.1)			
	(1.0,0.1)			



Table 6. Lynch Formulation (52)

	Formular Weight	Recommended Aqueous wt%
Na ₂ B ₄ O ₇ •10H ₂ O	381.37	0.35
NaNO ₃	84.80	0.1
NaNO ₂	69.00	0.05
Na ₂ SiO ₃ ·5H ₂ O	212.74	0.01
(NaPO ₃) xNa ₂ O		0.002
	167.25	0.001
	NaNO ₃ NaNO ₂ Na ₂ SiO ₃ · 5H ₂ O	Weight Na ₂ B ₄ O ₇ •10H ₂ O 381.37 NaNO ₃ 84.80 NaNO ₂ 69.00 Na ₂ SiO ₃ •5H ₂ O 212.74 (NaPO ₃) _x Na ₂ O

Total 0.513 wt.%



neck carried a dropping funnel containing 340 g(25 ml) of Hg. The flask was thoroughly flushed with N_2 , and 10 ml of Hg then was added. The flask was heated on an open flame until the start of the reaction. Additional Hg then was slowly added, with minimum additional heating. After the addition, the hot molten amalgam was poured onto a clean plate and broken up into pieces while still hot and brittle.

Amalgams containing less than 3 wt.* Na are not too sensitive to air; however they must be stored in an air-free atmosphere. Complete liquefaction occurs at following (liquidus) temperatures: 0.5% Na, 0 °C; 1.0% Na, 50 °C; 1.5% Na, 100 °C; 2.0% Na, 130 °C; 2.5% Na, 156 °C; 3% Na, 250 °C; 4.0% Na, 320 °C.

iii-2) Sodium Hyponitrite, Na₂N₂O₂ 9H₂O

The metal salts are generally prepared in variable yield by reduction methods, sodium amalgam being a favorite reducting agent:

$$2NaNO_3 + 8Na + 4H_2O = Na_2N_2O_2 + 8NaOH.$$

170.0 184.0 72 106.0 320.0

Sodium amalgam was added with stirring or shaking to an ice-cooled solution of 85 g of NaNO, in 250 ml of H₂O. The amalgam was prepared by dissolving 58 g of Na in 4000 g of Hg (1.43 wt.% Na). When three quarters of the amalgam had been added, the cooling was discontinued and the remainder of the amalgam was added at once. Shaking was continued for 10-15 mimutes, during which the temperature increased to 40 °C. When the temperature began to fall the mixture was poured into a closed flask with a narrow neck, then the first flask was rinsed with 2-3 ml of H₂O. The washings were combined with the main solution and the whole shaken vigorously for about ten minutes. The solution was decanted from the Hg and placed over H_2SO_4 in a vacuum desiccator at 35°C to 40°C in order to remove all the NH3. The $\mathrm{Na_2N_2O_2}$ 9 $\mathrm{H_2O}$ separated during this operation. It was suction-filtered on a fritted glass filter, washed with alcohol at a temperature above 10 °C to remove traces of NaOH, and dried in a desiccator.

Sodium Hyponitrite ($Na_2N_2O_2$ • $9H_2O$, 268.14) was small granular crystals or plates. It lost water of crystallization under vacuum.

IV. Experimental Results

A. Distilled Water and Sodium Chloride

Figure 8 shows the anodic polarization behavior of Al 7075-T6 in distilled water at room temperature. The profile is continuous with no discontinuity and may be adaptable to Tafel analysis and the corrosion current density can be found.

In Figure 9, anodic profile is presented for 0.1 wt.% NaCl at room temperature. The figure shows that this profile is continuous with no discontinuity. It is known that the corrosion potential of corroding 7075-T6 Al alloy depends strongly on the solution concentration, i.e, increasing corrosion potentials correspond to decreasing Cl concentration (82). With comparison of anodic polarization behavior between the distilled water and sodium chloride, the current density is increased by three orders of magnitudes.

B. Effects of Inhibitors

The effectiveness of inhibitors are based on the corrosion current density and pitting potential values obtained from the anodic polarization curves. The measure of an effective inhibition, therefore, is its ability to reduce the anodic reaction (corrosion) rate to an acceptably low level, and to raise the pitting potential to more



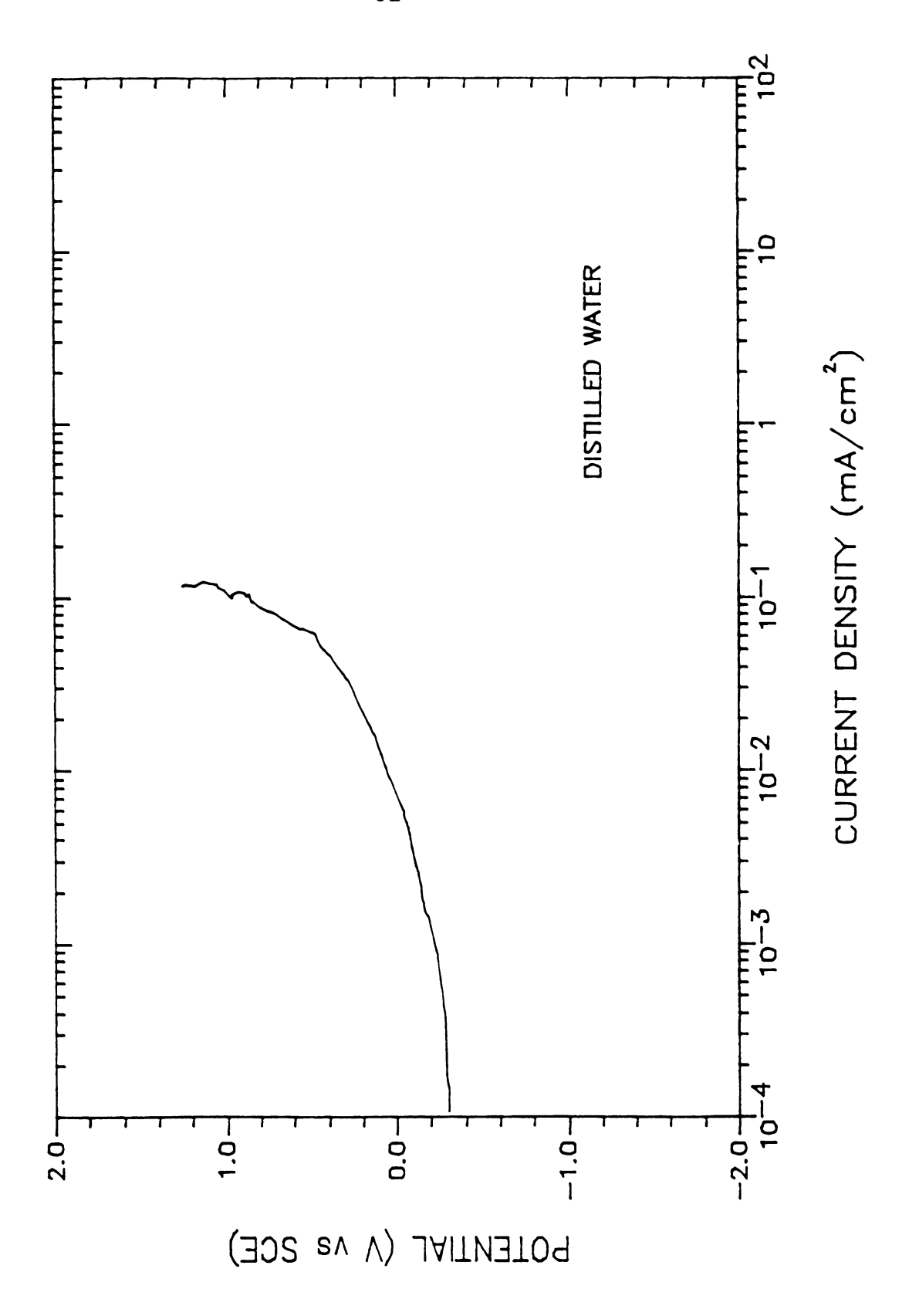


Figure 8. The Anodic Polarization of 7075-T6 Al Alloy in Distilled Water.

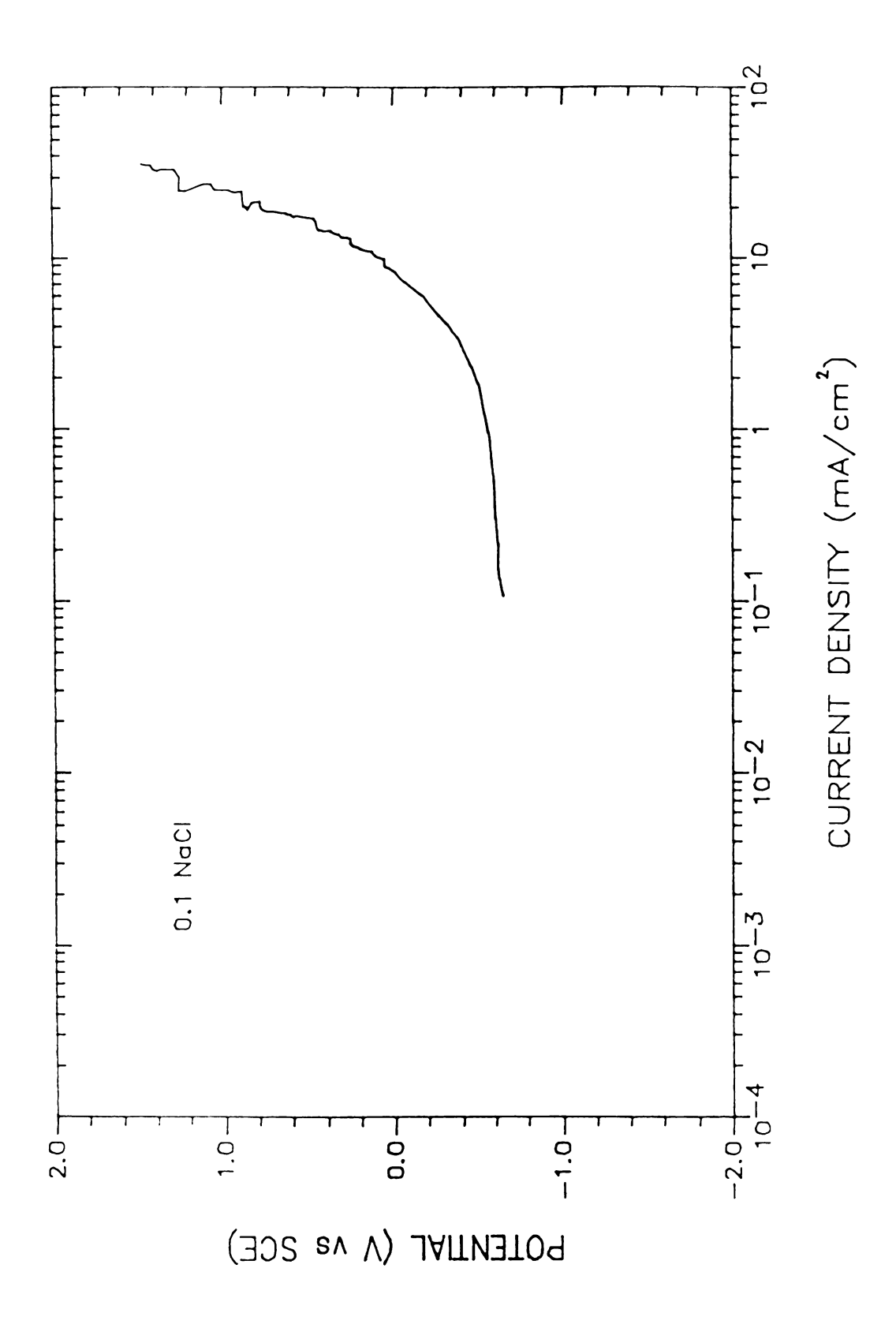


Figure 9. The Anodic Polarization of 7075-T6 Al Alloy in 0.1 wt.% Sodium Chloride.



positive value than the open circuit potential.

a) Sodium Nitrite, Borax and Lynch Formulation

Figure 10 shows the anodic polarization behavior of 7075-T6 Al alloy in inhibitor solutions for concentrations between 0.05 wt.% and 3.0 wt.% NaNO2. Sodium nitrite alone is an effective inhibitor but clearly exhibits a reverse effect at concentrations above 0.1 wt.% where corrosion currents increase. Figure 11 shows the effect of concentration of nitrite on current density at constant potential (0.2 V). In the presence of sodium chloride, sodium nitrite has no useful inhibitive properties (Figure 12). However, at high concentration (8 wt.%) it has the good inhibition. This may suggest that the passive film formed by NaNO2 at low concentration is still weak and ineffective against chloride attack.

Figure 13 shows the anodic polarization behavior of 7075-T6 Al alloy in the inhibiting solution for concentrations between 0.1 wt.% and 3.0 wt.% Na₂B₄O₇ with 0.1 wt.% NaNO₂. When coupled with borax, the passivating effect of 0.1 wt.% NaNO₂ is slightly diminished by about one order of magnitude, but still is effective.

As shown in Figure 14, addition of 0.1 wt.% NaCl, however, essentially cancels the inhibitive effects, although a small passivity zone is present. There are no



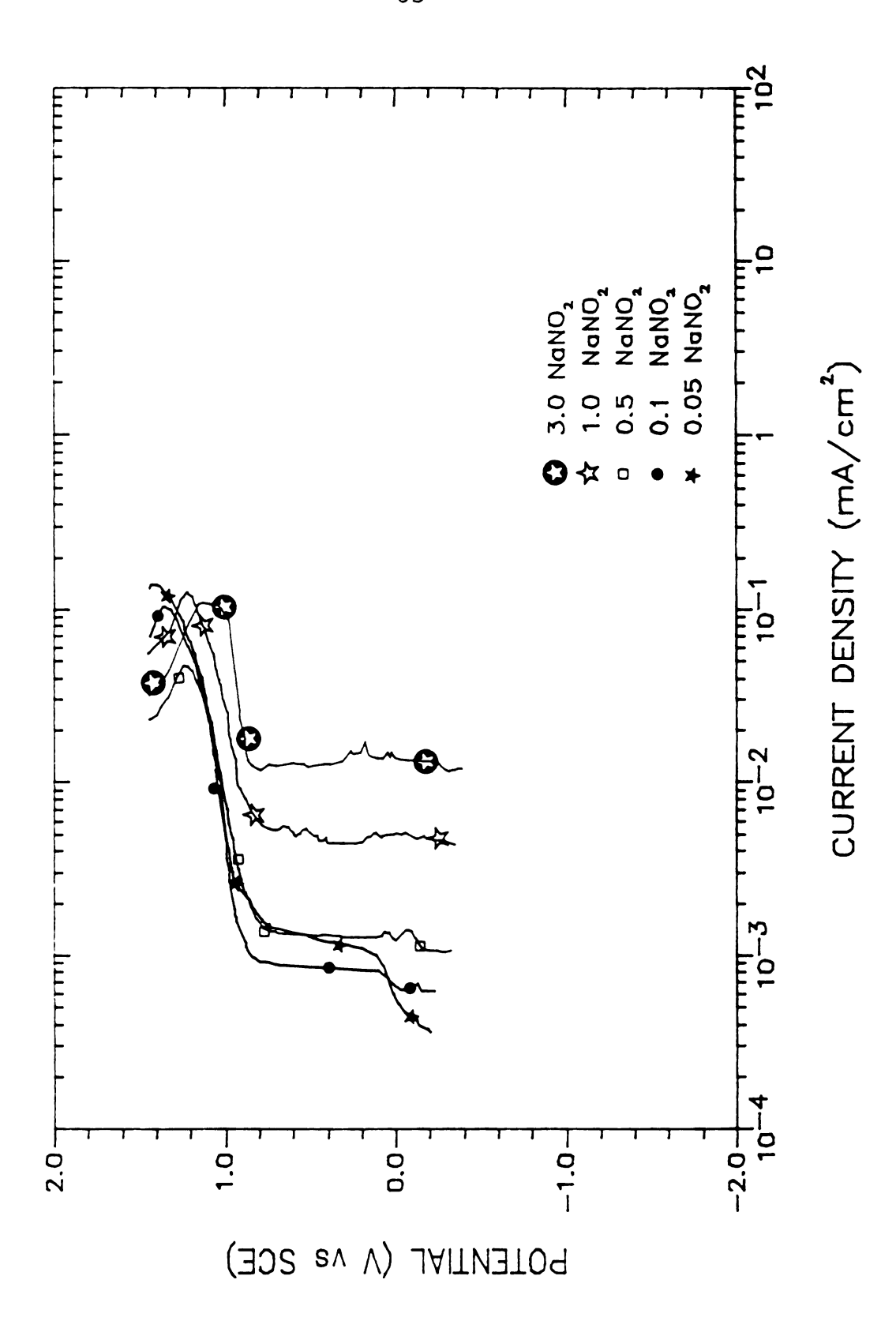


Figure 10. The Anodic Polarization of 7075-T6 Al Alloy in Sodium Nitrite.

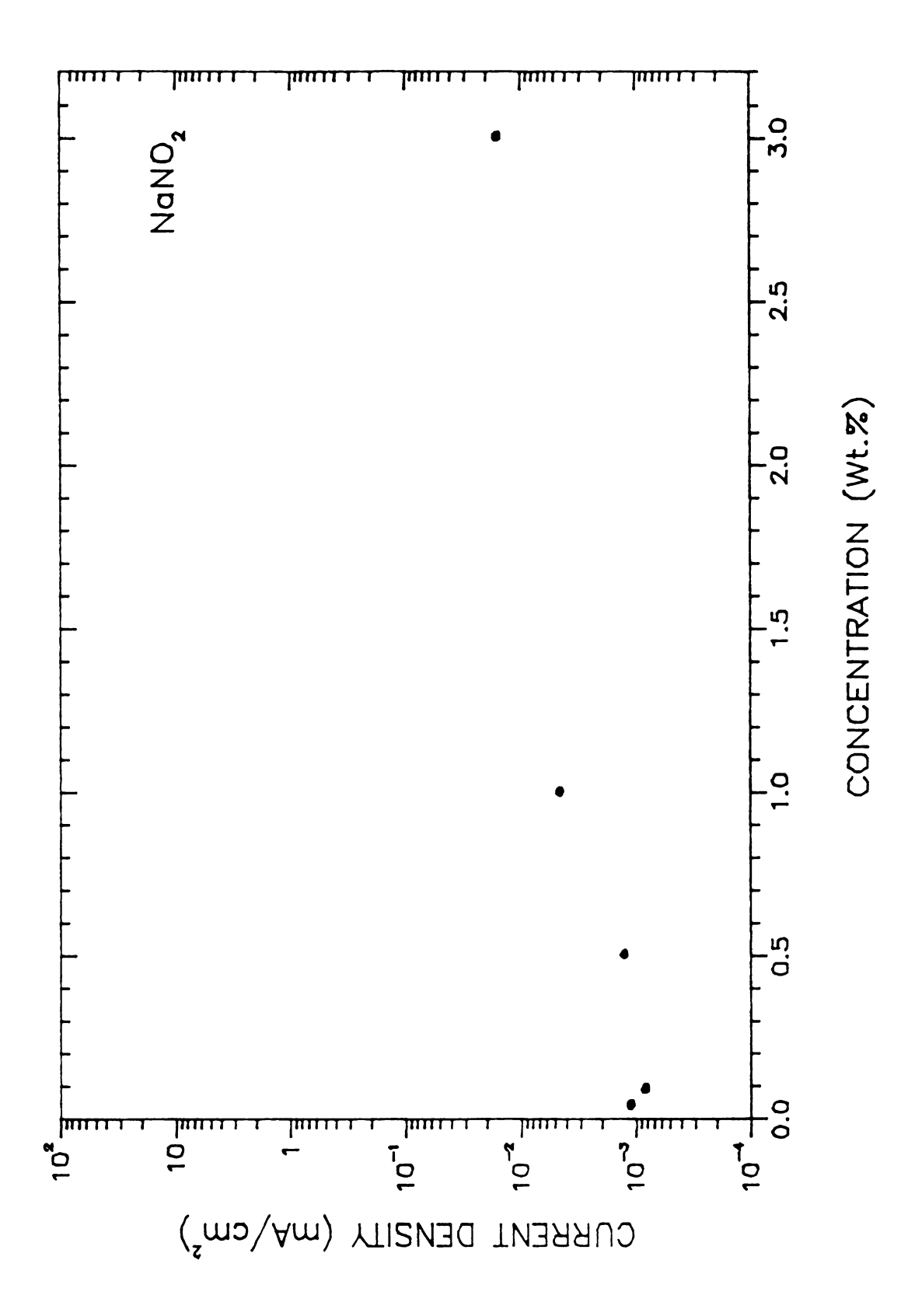


Figure 11. The Effect of Concentrations of Nitrite on Current Density at Constant Potential.

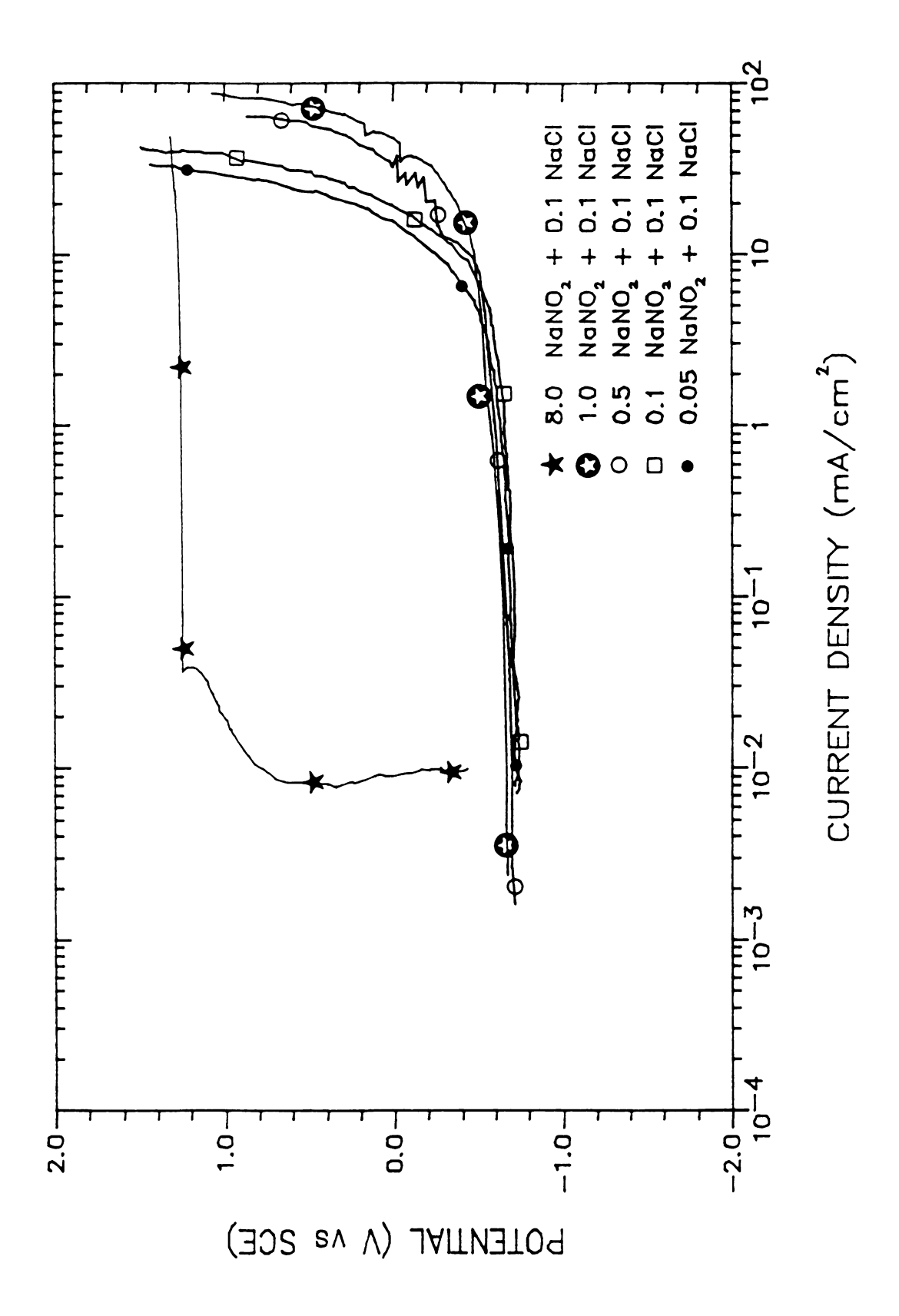


Figure 12. The Anodic Polarization of 7075-T6 Al Alloy in Sodium Nitrite with Sodium Chloride.

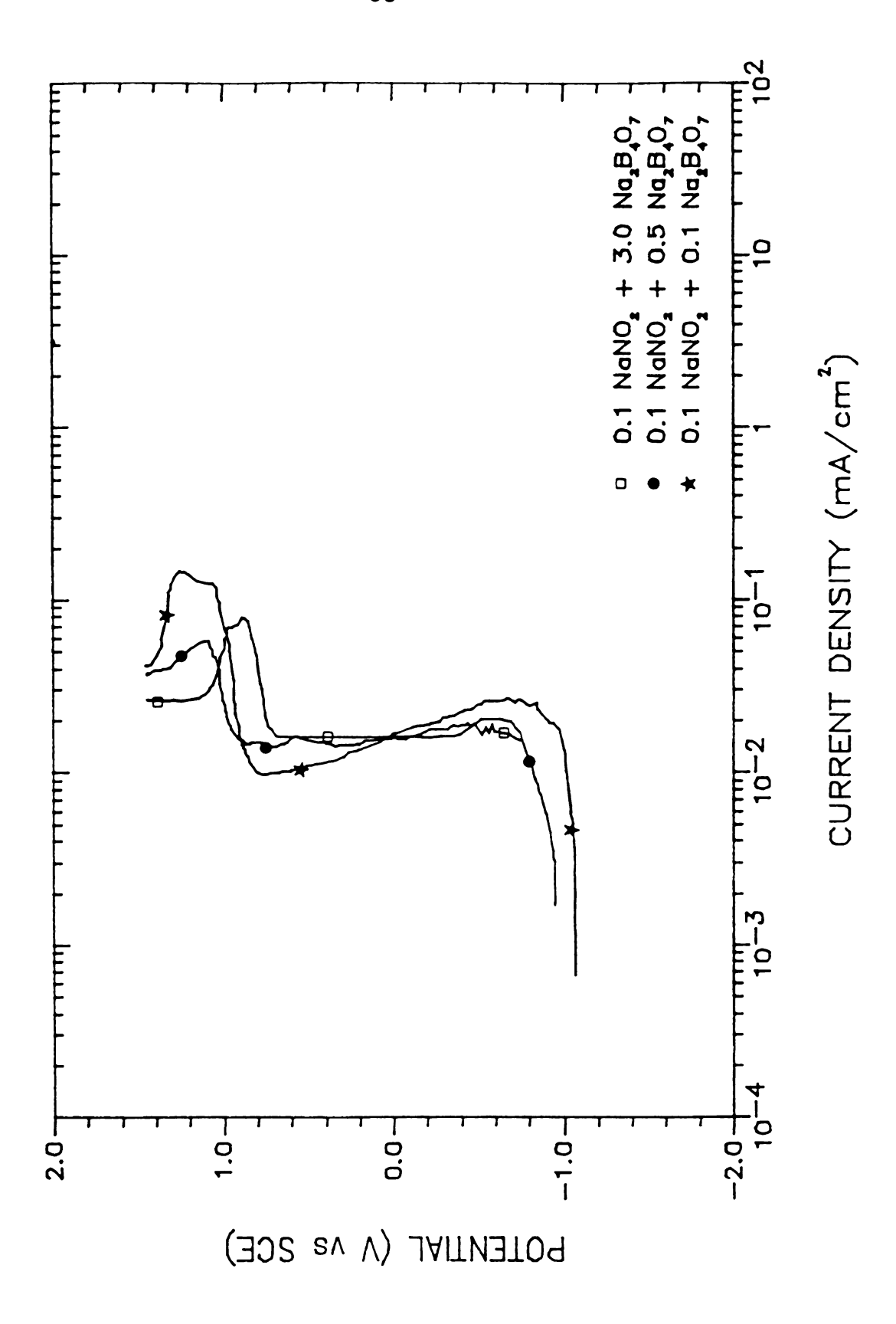


Figure 13. The Anodic Polarization of 7075-T6 Al Alloy in Sodium Nitrite and Borax.

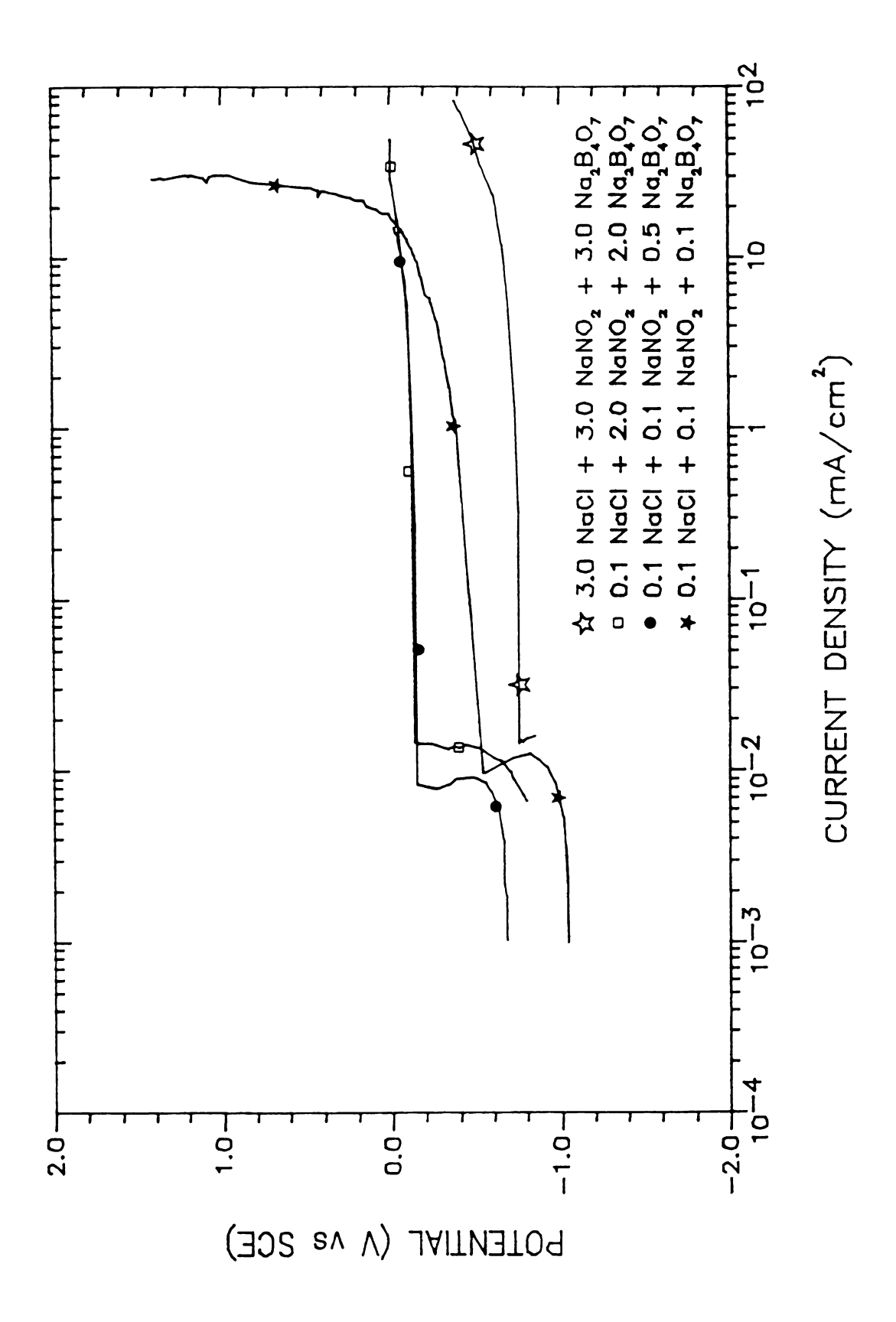


Figure 14. The Anodic Polarization of 7075-T6 Al Alloy in Sodium Nitrite and Borax with Sodium Chloride.



significant changes despite of addition of higher concentration.

Figure 15 shows the anodic polarization behavior of 7075-T6 Al alloy in the inhibition solution of Lynch formulation. When compared with 0.1 wt.% NaNO₂, the current density of passivity in the 0.513 wt.% Lynch formulation is a little larger than one in the 0.1 wt.% NaNO₂ and the pitting potential is lower. Rather, these values are almost the same as in 0.5 wt.% NaNO₂. According to Figure 16, addition of NaCl essentially cancels the inhibitive effects, although there is some passive region over the potential range of about 200 mV.

With comparison of Figure 14, the pitting potential of Lynch formulation is between that in the 0.1 wt.% borax and 0.5 wt.% borax although the passive current density is smaller than the above borax concentration.

Figures 17 and 18 show the cathodic polarization behavior of 7075-T6 Al alloy in solution for concentration between 0.05 wt.% and 0.5 wt.% NaNO₂ with and without 0.1 wt.% NaCl, respectively. According to these results, the current density is increasing with decreasing potential. These results show that sodium nitrite has no effective inhibition for the cathodic reaction.



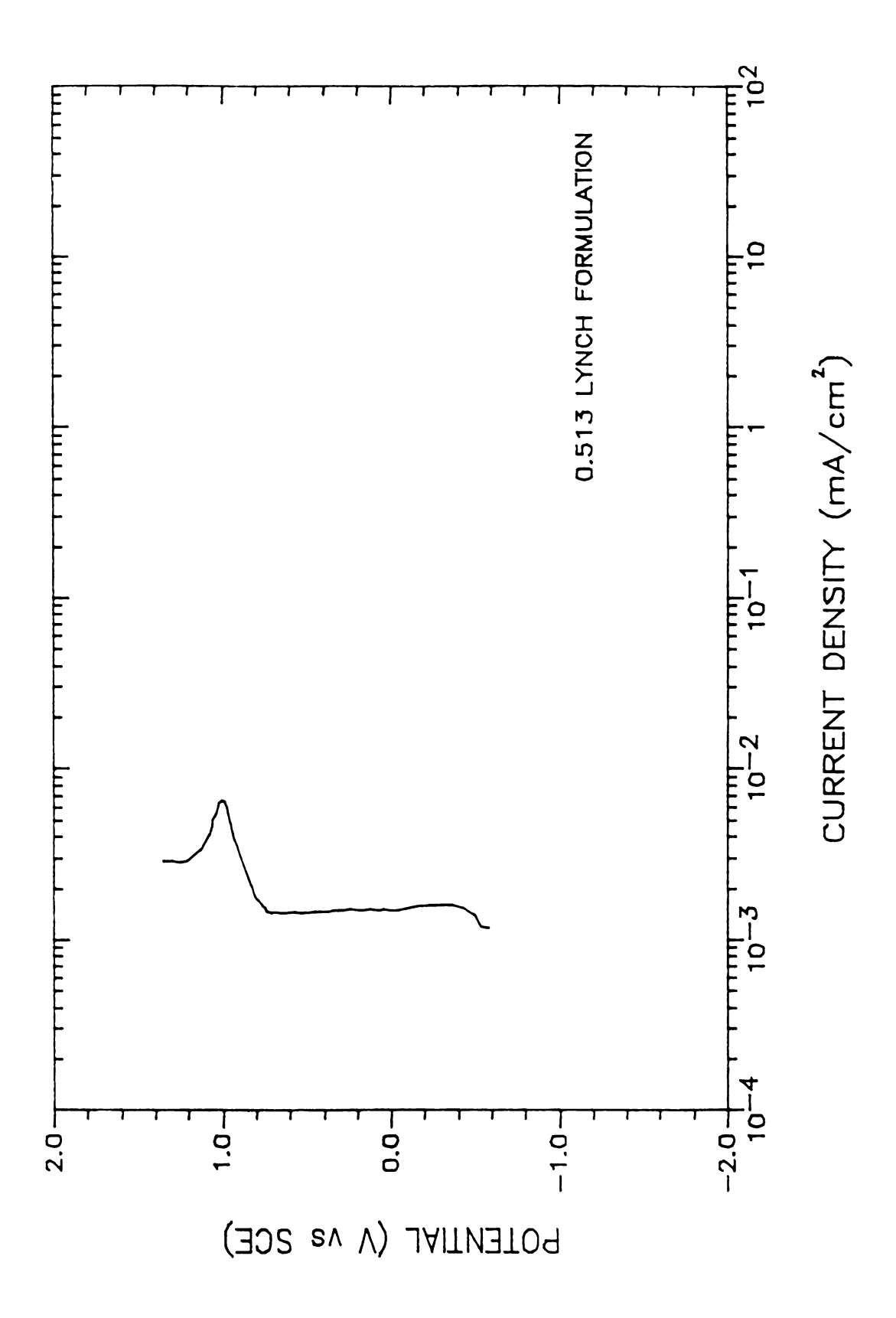


Figure 15. The Anodic Polarization of 7075-T6 Al Alloy in Lynch Formulation.

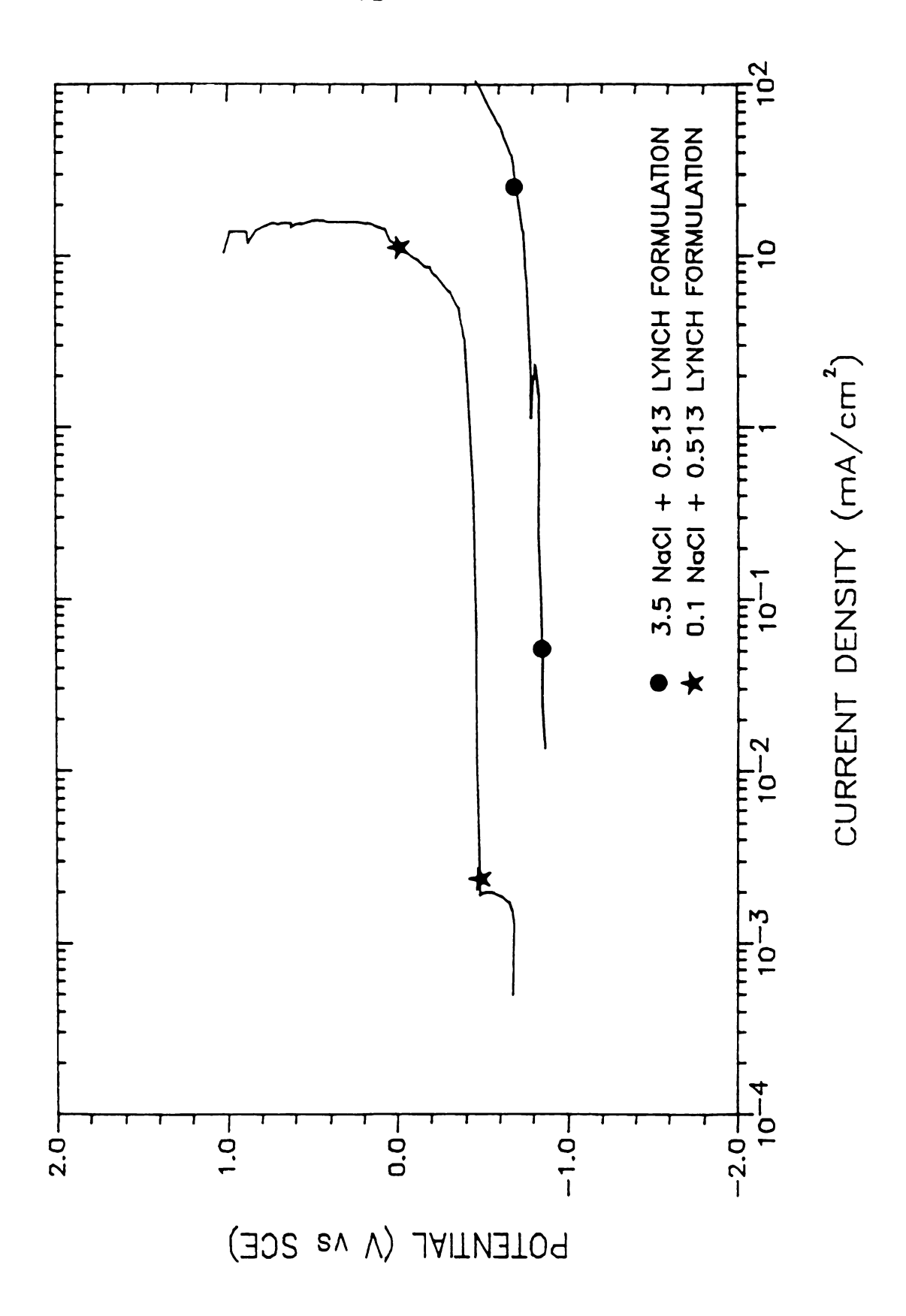


Figure 16. The Anodic Polarization of 7075-T6 Al Alloy in Lynch Formulation with Sodium Chloride.

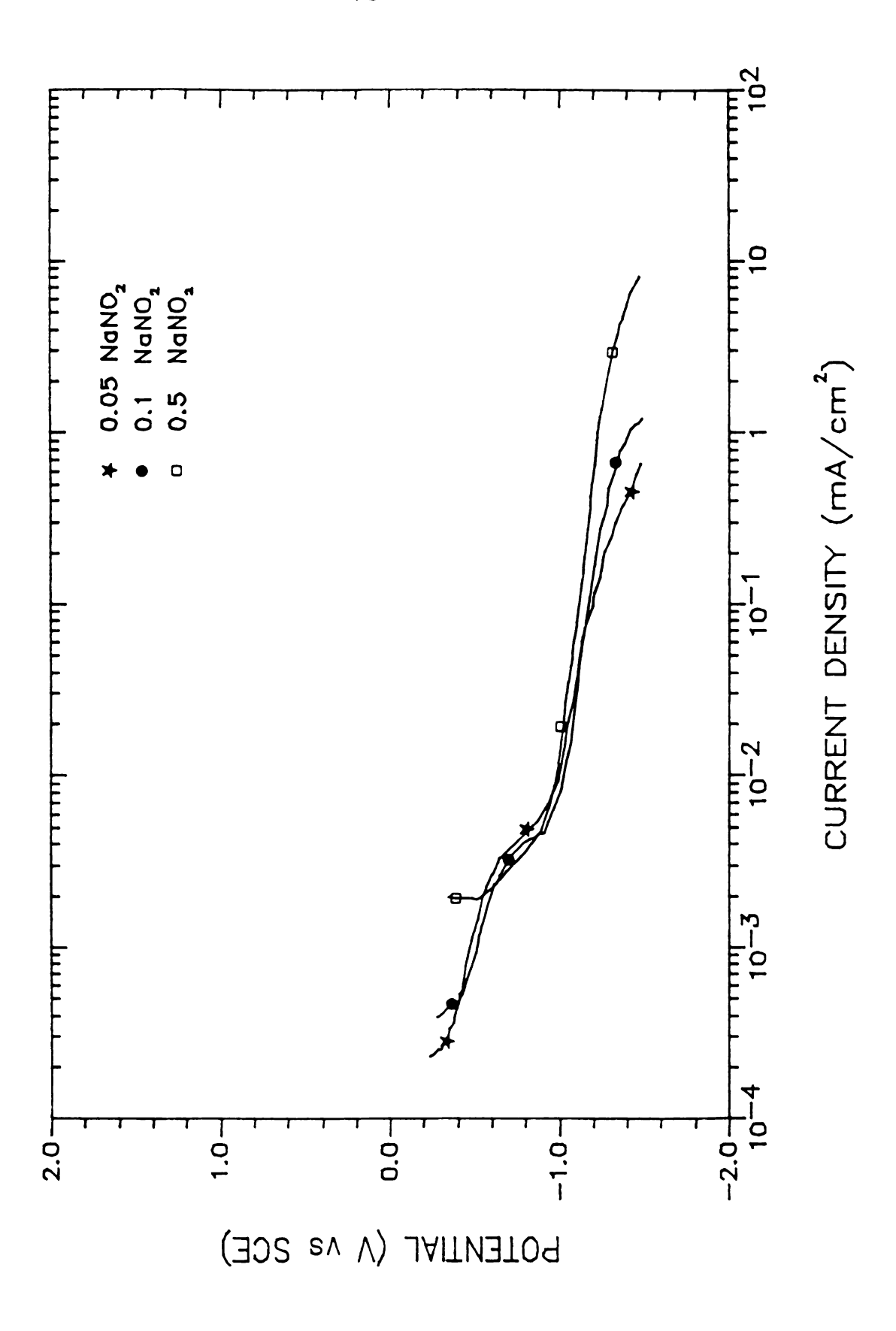


Figure 17. The Cathodic Polarization of 7075-T6 Al Alloy in Sodium Nitrite.

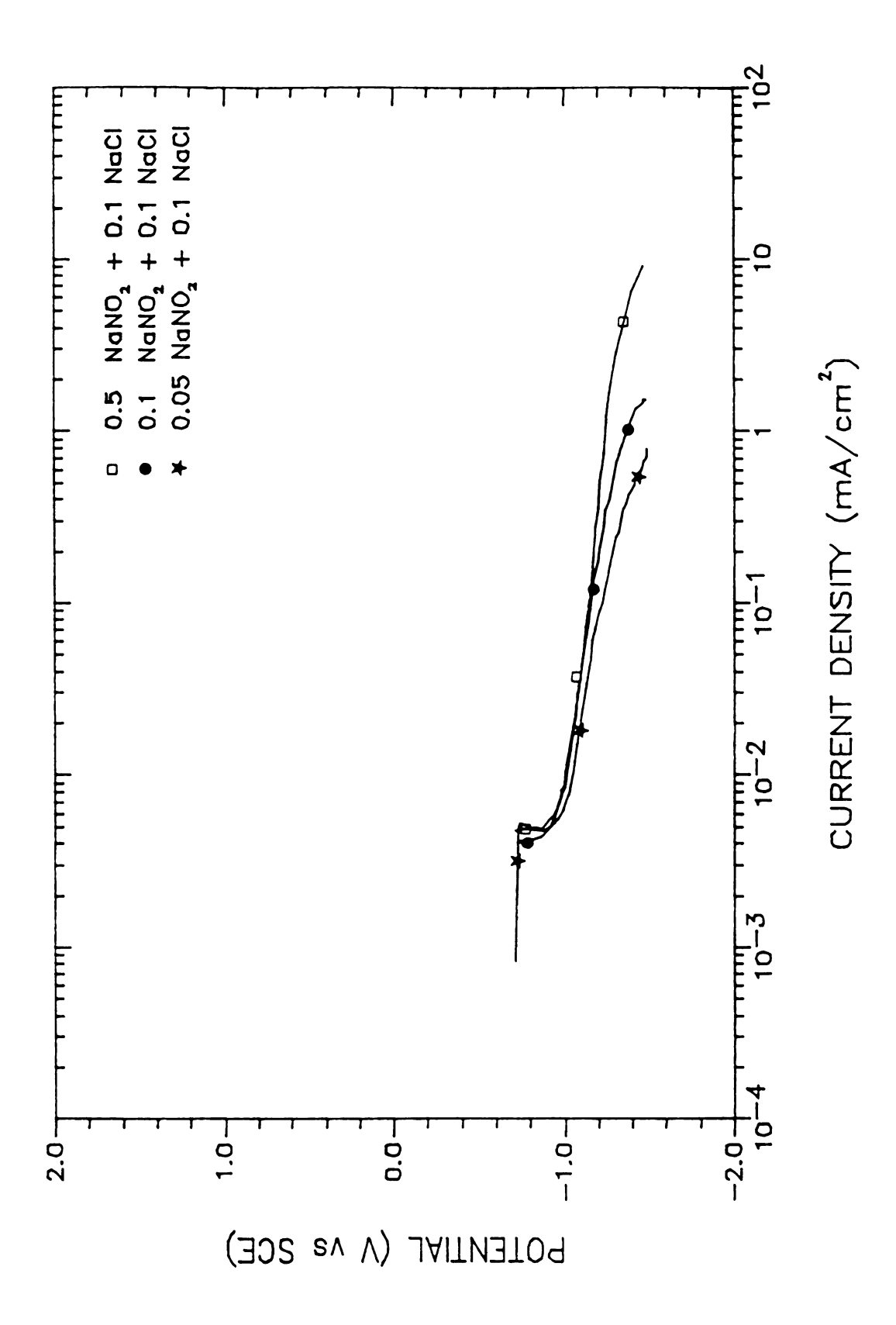


Figure 18. The Cathodic Polarization of 7075-T6 Al Alloy in Sodium Nitrite with Sodium Chloride.

It has been found $^{(83)}$, $^{(84)}$ that NaNO₂ and the combination of NaNO₂ and Na₂B₄O₇ are effective to eliminate the environmental assisted crack growth in the aggressive aqueous solution, e.g., sodium chloride for high strength steels. The nitrite ion affects the potential, that is, those salts whose anions have high redox potential. For example,

$$NO_2^- + 8H^+ + 6e = NH_4^+ + 2H_2^0$$
,
E = + 0.90 V SHE.

b) Sodium Nitrate

Figures 19 and 20 show the anodic polarization behavior of 7075-T6 Al alloy in solution for concentrations 0.05 wt.% - 8.0 wt.% NaNO3 and 0.05 wt.% - 1.0 wt.% NaNO3 with and without 0.1 wt.% NaCl, respectively. These results indicate that sodium nitrate is an effective inhibitor, but exhibits a reverse effect (except 1.0 wt.%). Figure 21 shows the effect of concentration of nitrate on current density at constant potential (0.2 V). In the presence of sodium chloride, sodium nitrate has effective inhibition. At the concentration up to 0.1 wt.% NaNO3, there is no effective inhibition as with the NaNO2. It begins to show effective inhibition, however, as the concentration of NaNO3 is increased above 0.1 wt.%. Comparing between 1.0 and 8.0 wt.% NaNO3 with sodium chloride shows similar

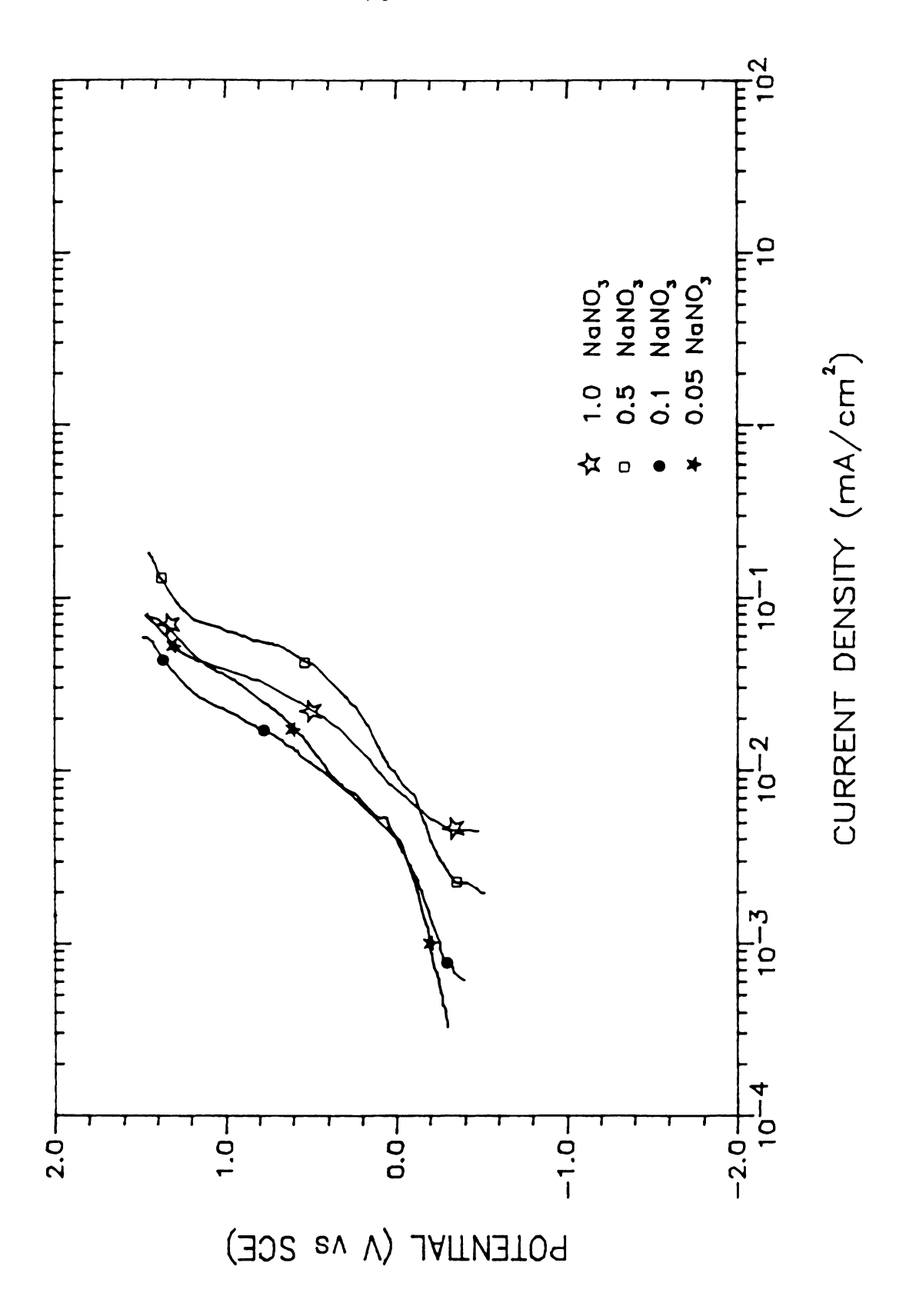


Figure 19. The Anodic Polarization of 7075-T6 Al Alloy in Sodium Nitrate.

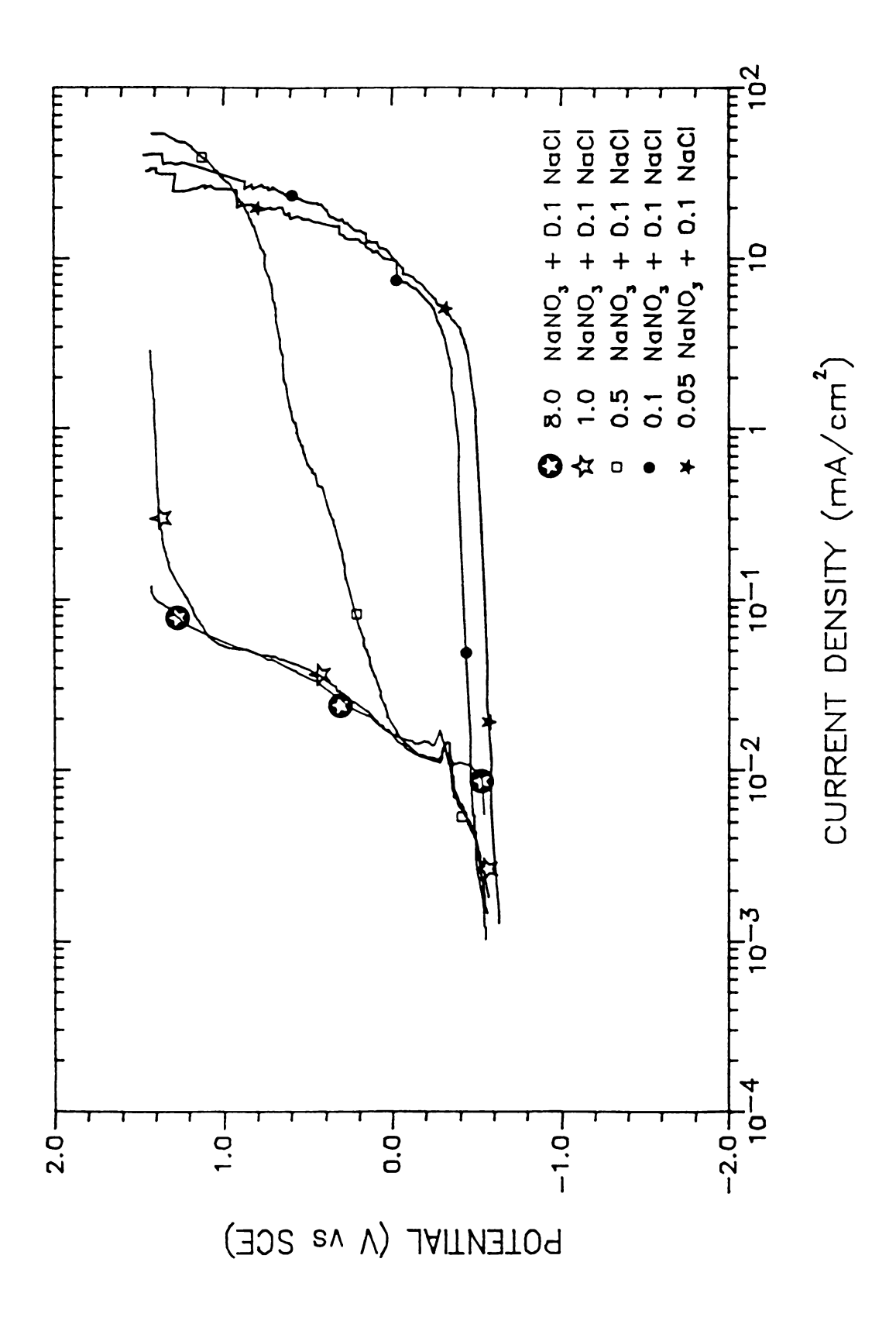


Figure 20. The Anodic Polarization of 7075-T6 Al Alloy in Sodium Nitrate with Sodium Chloride.

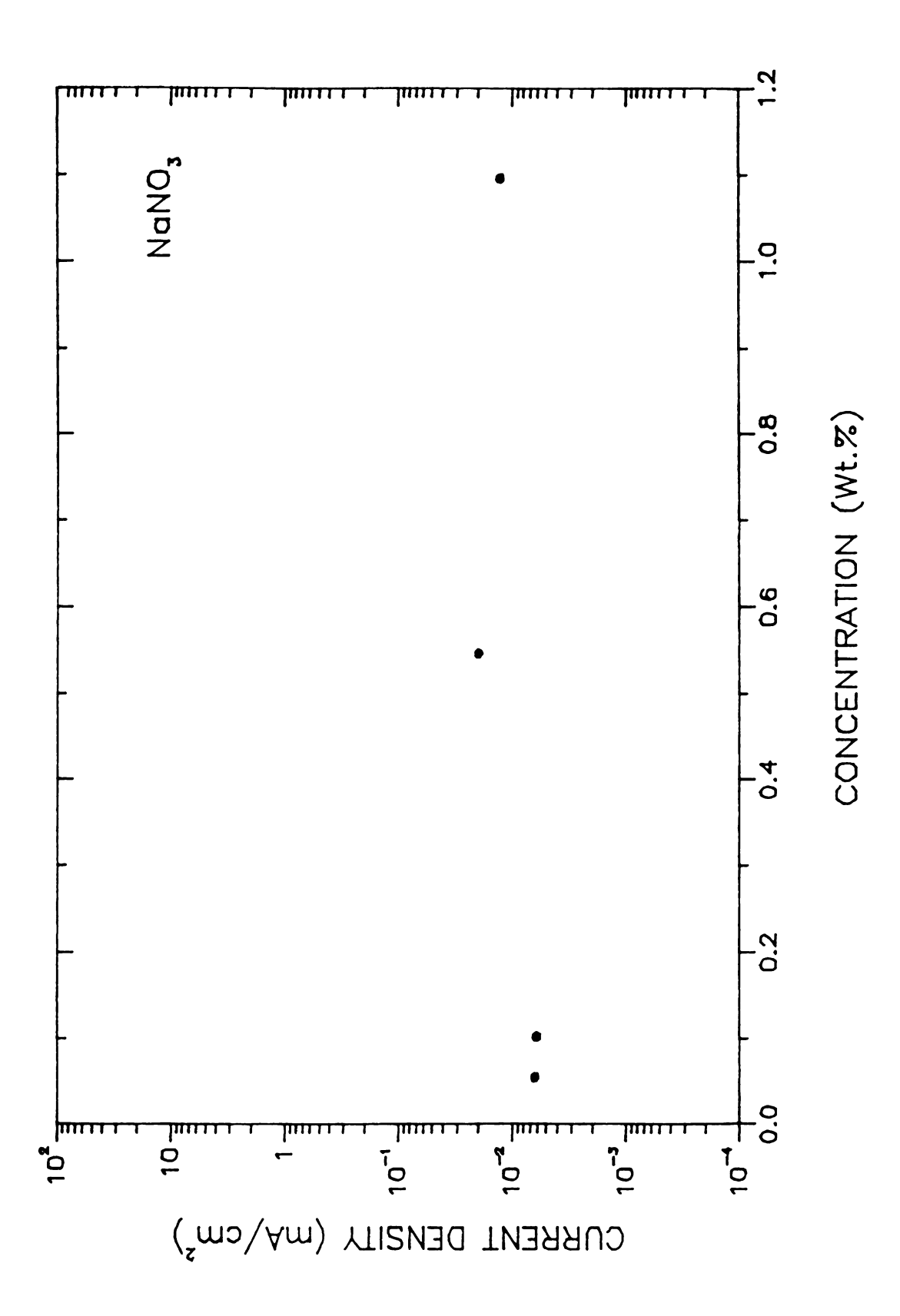


Figure 21. The Effect of Concentrations of Nitrate on Current Density at Constant Potential.



behavior, but the pitting potential of 8 wt.% NaNO_3 is a little greater than that of 1.0 wt.% NaNO_3 , i.e., there is wider passivity region in 8 wt.% NaNO_3 , which indicates that passivity in 8 wt.% NaNO_3 is much stronger. When compared with NaNO_2 and NaNO_3 , the effective inhibition of NaNO_2 is larger than that of NaNO_3 without sodium chloride. In the presence of sodium chloride, however, the inhibition of NaNO_3 is larger than that of NaNO_2 and the pitting potential of NaNO_3 is higher than that of NaNO_2 .

c) Sodium Hyponitrite

Figures 22 and 23 show the anodic polarization behavior of 7075-T6 Al alloy in the inhibition solution for concentration between 0.05 wt.% and 0.5 wt.% Na₂N₂O₂ with and without sodium chloride. The results indicate that the hyponitrite has a strong passivating effectiveness on 7075-T6 Al alloy. Pitting potential of 0.5 wt.% Na₂N₂O₂ in the presence of chloride ion is increased remarkably. When compared with sodium nitrite and sodium nitrate, the inhibition in the solution of hyponitrite is less effective than that in the sodium nitrite. Although the passivation is destroyed in the presence of sodium chloride, the region of the passivity becomes wider with increasing concentration of sodium hyponitrite, that is, passivation is lost at a significantly higher potential.

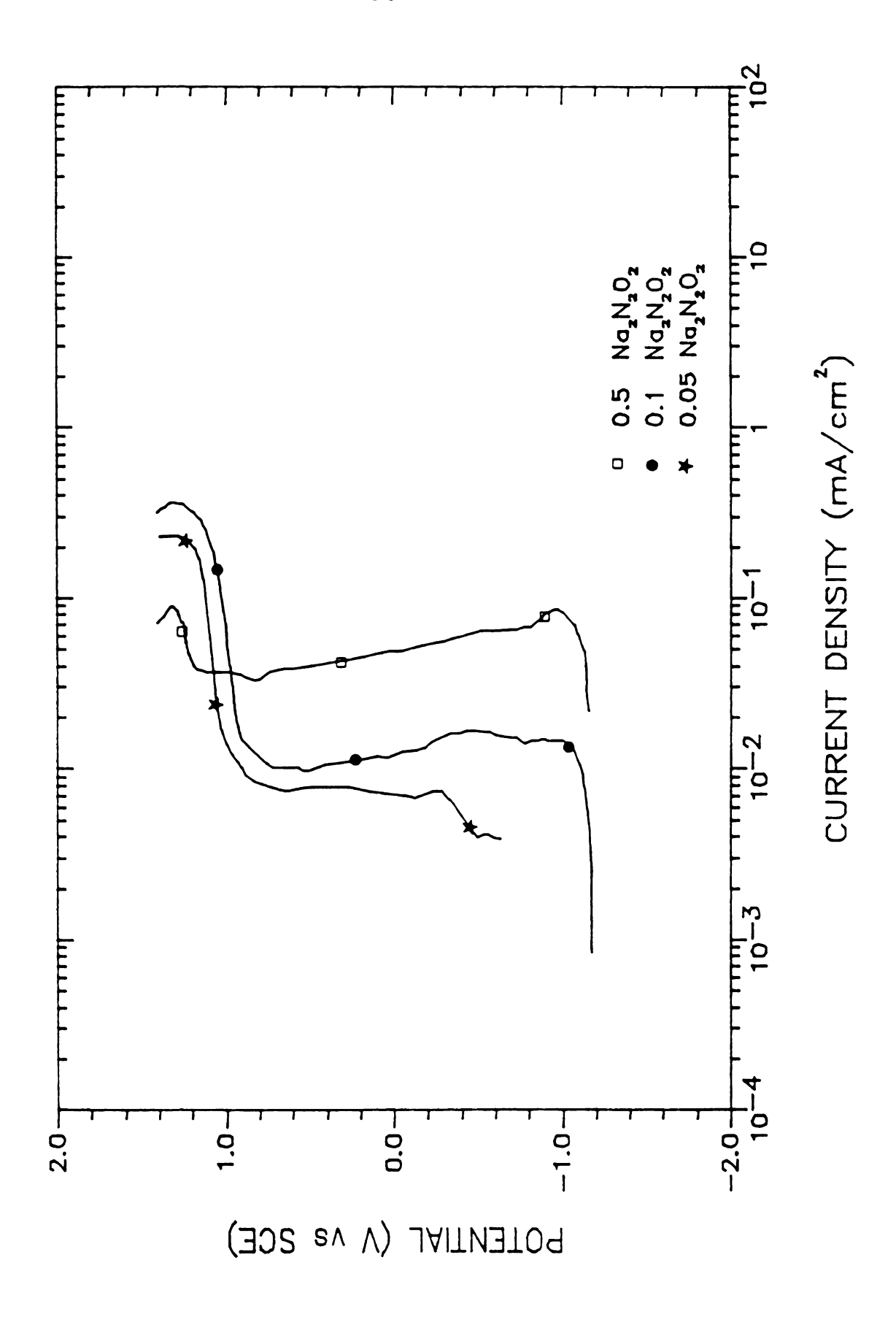


Figure 22. The Anodic Polarization of 7075-T6 Al Alloy in Sodium Hyponitrite.

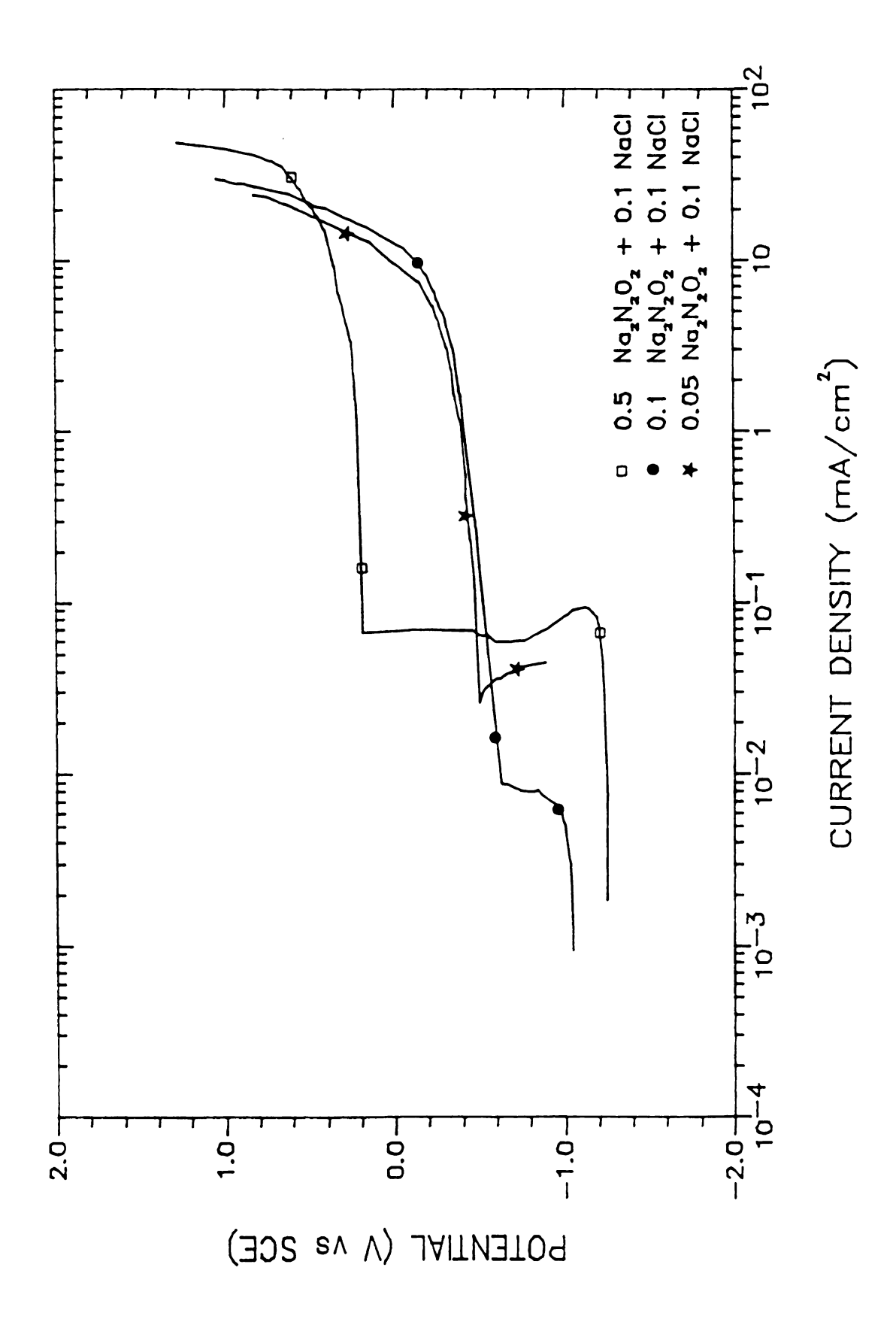


Figure 23. The Anodic Polarization of 7075-T6 Al Alloy in Sodium Hyponitrite with Sodium Chloride.

d) Ammonium Hydroxide

Figure 24 shows the anodic polarization behavior of 7075-T6 Al alloy in solution for concentration between 0.05 wt.% and 1.0 wt.% NH₄OH. The result shows that ammonium hydroxide has a strong passivating effectiveness on 7075-T6 Al alloy although the inhibition is less effective than that of sodium nitrite, as is the case with sodium hyponitrite. In the presence of sodium chloride, the passivator is effectively destroyed, as also is true for the case of sodium hyponitrite, while passivation is lost at a higher potential with the concentration of ammonium hydroxide (Figure 25).

C. Effects of Temperature

a) Sodium Nitrite

Figure 26 shows that the current density of passivity generally increases with temperature except at 25° C and 50° C. The pitting potential at 25° C is the highest and decreases with the temperature.

b) Sodium Nitrate

In Figure 27, the current density of aluminum in the presence of sodium nitrate increases with the temperature.

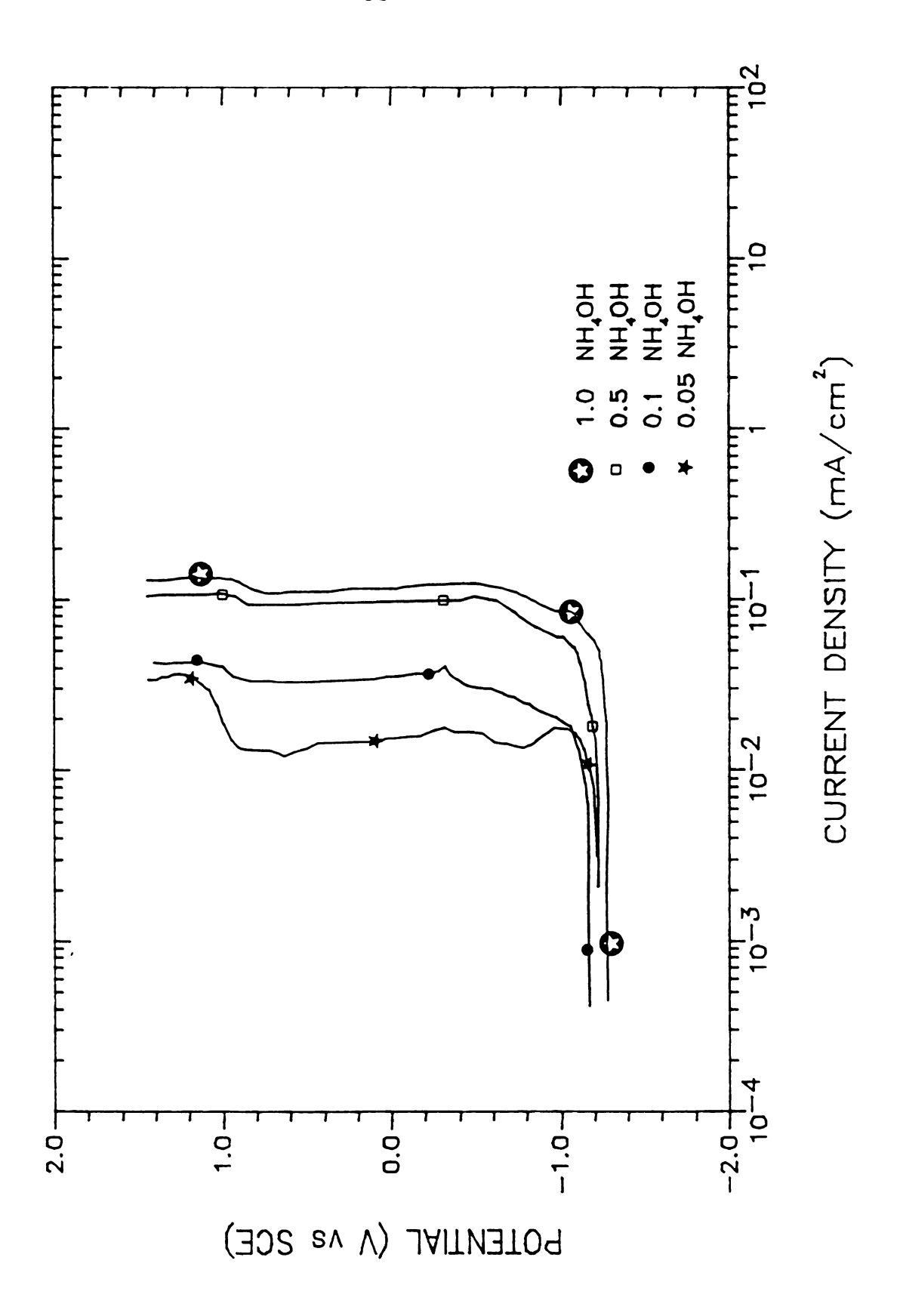


Figure 24. The Anodic Polarization of 7075-T6 Al Alloy in Ammonium Hydroxide.

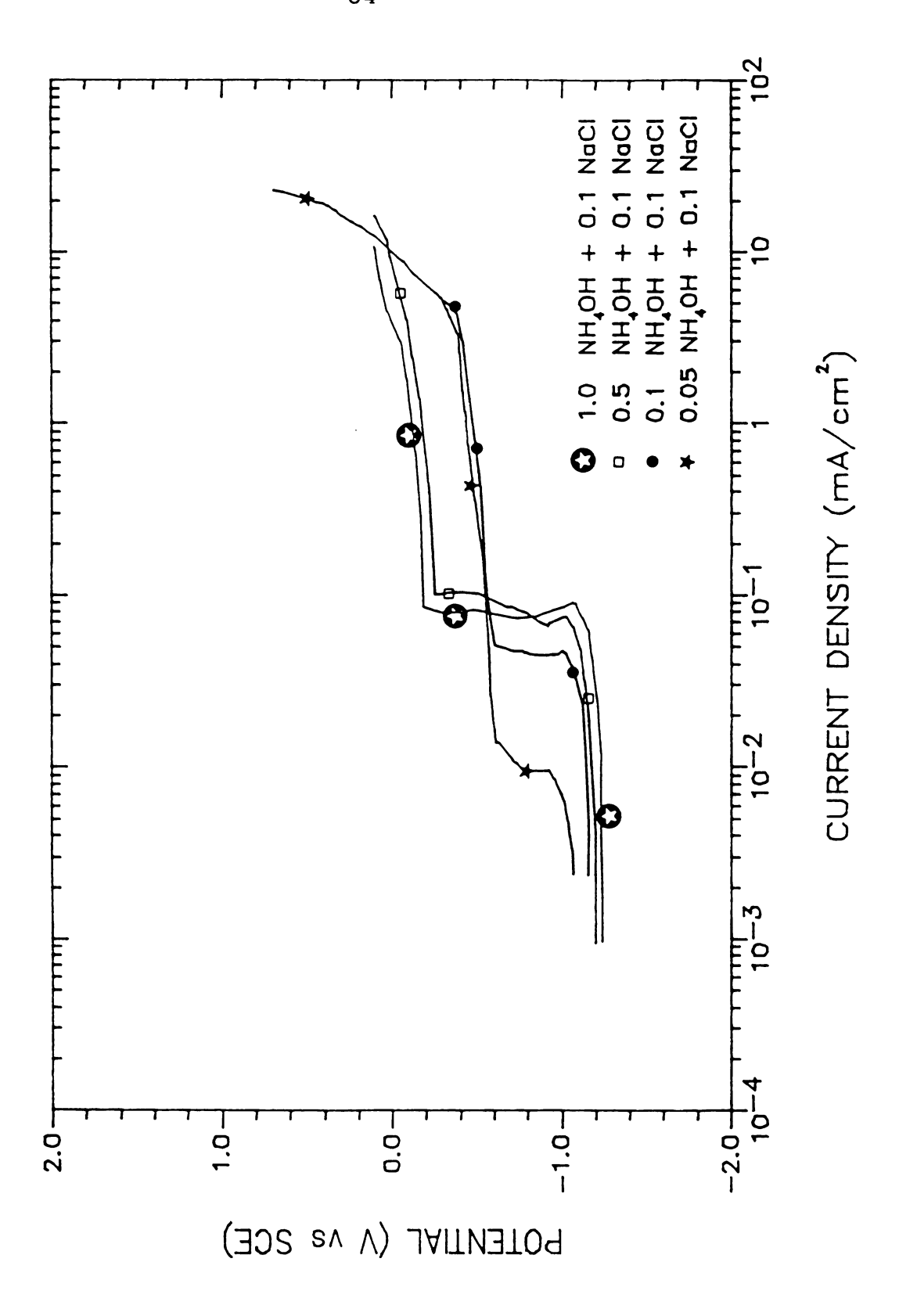


Figure 25. The Anodic Polarization of 7075-T6 Al Alloy in Ammonium Hydroxide with Sodium Chloride.

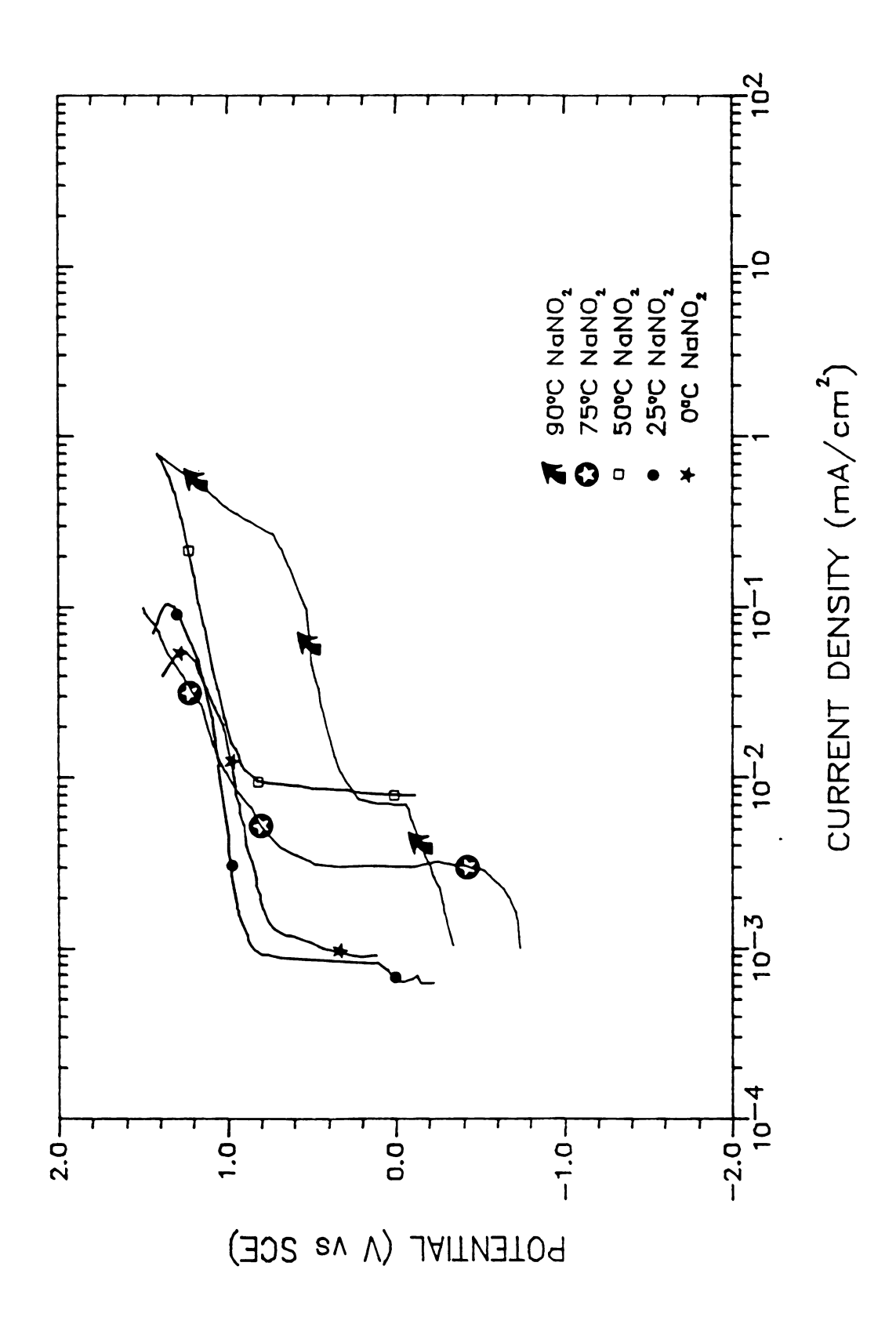


Figure 26. The Anodic Polarization of 7075-T6 Al Alloy in Sodium Nitrite vs. Temperature.

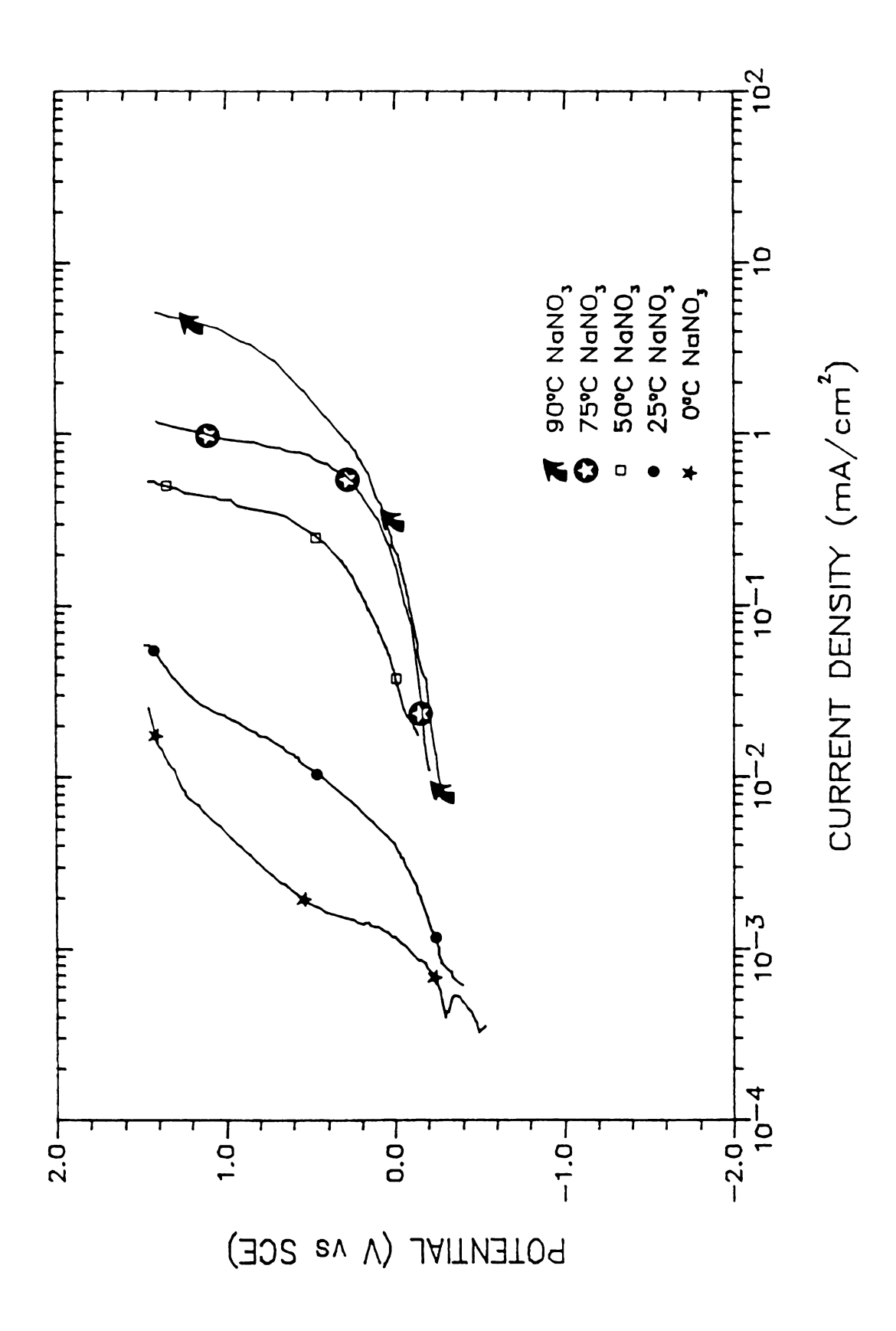


Figure 27. The Anodic Polarization of 7075-T6 Al Alloy in Sodium Nitrate vs. Temperature.

That is, the current density increases as the temperature is raised to $50 - 75^{\circ}$ C, whereas above this temperature, the current density seems to be constant.

V. Discussion

In water, aluminum reacts to form aluminum hydroxide and hydrogen:

$$2A1 + 6H_2O = 2A1(OH)_3 + 3H_2$$
 (a)

This also is the reaction that produces the thickened surface film in water. The corrosion product, Al(OH)₃ has a very low solubility in water, and precipitates immediately.

The surface film formed in water is hydrated aluminum oxide ($Al_2O_3 \cdot xH_2O$). The degree of hydration (x) depends on the temperature. The film is mainly Bayerite ($Al_2O_3 \cdot 3H_2O$) below about 75°C while it is mainly Boehmite ($Al_2O_3 \cdot H_2O$) above this temperature (85).

Whether localized corrosion develops depends on the rates of film breakdown and film repair, both of which are influenced by the nature of ions present, as well as by the microstructure of the surface.

The four steps (39) by which aggressive ions act on Al is generally accepted. The first step of them is adsorption of aggressive ions on the oxide covered aluminum. Corrosion

of Al and 7075-T6 Al alloy at the bare surface in solutions containing dilute NaCl is accompanied by the adsorption of anions, e.g., Cl that would promote pitting corrosion. There is evidence for the adsorption of anions, especially, for the adsorption of chloride as indicated by Videm (86) and Berzin (45). The pickup of chlorine-36 on oxide-covered aluminum surface by autoradiography before film breakdown and during the pitting corrosion process (86), and the adsorption isotherm on corroding Al with $^{36}\text{Cl}^-$ (45) have been reported. It has been suggested that the site of anion adsorption will be at a flaw or dislocation in the oxide $film^{(87),(88)}$. Foroulis, et al⁽⁴⁶⁾ discussed the ratedetermining steps depending on chloride concentrations. In low chloride concentrations, adsorption of chloride ions from solution on the hydrated aluminum oxide surface is likely to become the rate-determining step in the process of passivity breakdown, while in the high chloride ion concentration, the reaction step resulting in formation and dissolution of the hydroxylchloride aluminum salt is likely to be the rate-determining step in the process of pit initiation.

The second step is the chemical reaction of the adsorbed anion with the aluminum ion in the aluminum oxide. At this step, stoichiometric compounds are formed by chemical reaction. The most probable reaction mechanism

accompanying the initial stage of the corrosion process of 7075-T6 Al alloys in NaCl is (49):

$$Al = Al^{3+} + 3e$$
 (b)

$$Al^{3+} + H_2O = H^+ + AlOH^{2+}$$
 (c)

$$A1^{3+} + C1^{-} = A1C1^{2+}$$
 (d)

$$AlOH^{2+} + 2H_2O = Al(OH)Cl^+$$
 (e)

$$Al(OH)Cl^{+} + H_{2}O = Al(OH)_{2}Cl + H^{+}$$
 (f)

$$Al(OH)_2Cl + H_2O = Al(OH)_3 + H^+ + Cl^-$$
 (g)

$$Al(OH)_{3(amorphous)} = Al_2O_3 \cdot H_2O$$
 (h)

It is believed that the hydrated aluminum ion, $Al(H_2O)_6^{3+}$ is rapidly formed, equilibrium being achieved in about 1 μ sec. The hydrated Al^{3+} ion undergoes a very fast hydrolysis reaction written as Equation (c). Both of the Al^{3+} and $Al(OH)^{2+}$ can react with Cl^- according to Equations (d) and (e).

The reaction (e) has an equlibrium constant of K=3.3 and its activation energy is 4.25 kcal, suggesting a diffusion-controlled reaction, while the reaction (d) has an equlibrium constant of K=3.0 and activation energy for the reaction (d) is 12.3 kcal, suggesting a chemical reaction. Both the Al(OH)Cl⁺ and AlCl²⁺ are in equlibrium.

Reaction (e) is faster than reaction (d). It may be suggested that both reactions (d) and (e) may take place as an anodic dissolution mechanism.

The basic aluminum chloride is converted slowly to amorphous, Al(OH)₃, which has a free energy of formation of - 271.9 kcal, and is tranformed to the stable hydrated oxide which has a free energy of formation of - 436.3 kcal. The conversion of amorphous alumina to hydrated aluminum oxide, reaction (h), also is explained by change in electrical properties of the anodically formed film (89), (90).

The third step is the thinning of the oxide film by dissolution. In the chloride solution, chloride is characterized by its ability to penetrate the oxide film, i.e., to diffuse chloride through the aluminum oxide lattice, or to form soluble compounds or transitory species. If the oxide film on the aluminum surface were completely uniform, both physically and chemically, it would be expected that the thinning would be uniform over the whole surface. If not, it would be expected that the dissolution process would take place at oxide imperfections. The flaws would be the preferred sites for adsorption and then for accelerated film thinning.

The last step is the direct attack of the exposed metal by the aggressive anion. Once the film is sufficiently thinned, metallic aluminum is attacked rapidly and a pit is propagated. The attack on the metal will also be concentrated because the film is thinned locally. The direct attack on the metal surface is not a smooth, continuous reaction. Rather, it is an erratic process and becomes apparent in the potential cycling as indicated by Hagyard, et al (91) who observed fluctuation of the potential of the aluminum electrodes. It is microscopically observed that the pit formed on 7075 Al alloy in halide solutions (except fluoride) is predominantly hemispherical (92). The propagation rate is expressed in terms of current as a function of time.

$$i - i_p = a(t - t_i)^b$$

where i = the dissolution current, i_p = the passive current, t = time, t_i = induction time, a = a constant dependent on the halide solution, and b = a constant dependent on the geometry of the pit. Dalleck showed that the behavior of aluminum alloy was cubic behabior experimentally, i.e.

$$(i - i_p) = 0.0051(t - t_i)^3$$
 for 4 x 10⁻³ N Cl⁻.

During the last step, the heterogeneity of the alloy leads to accelerated attack. In an AlZnMg (7075 - T6 Al alloy), Mg and Zn are heavily segragated at grain boundary. The free Mg can be incorporated into the corrosion product film in the form of MgH or MgH₂ compounds with the hydrogen produced by the reaction of aluminum with water. The formation of these compounds may prevent the formation and discharge of molecular hydrogen, giving the atomic hydrogen enough time to diffuse into the metal and produce embrittlement.

The model to stability and breakdown of the passivity proposed (93). In this model, it is assumed that the passive film is a hydrated oxide film having a gel-like structure as indicated in Figure 28-a. The anodic polarization pulls out the proton included in the film structure. The metal ions produced by the anodic dissolution through an undeveloped part in the film from intermediates is denoted as MOH+. The MOH+ is captured by surrounding H20 molecules and precipitates as a solid film in the undeveloped part (Figure 28-a'). Since deprotonation might create a high field at the vacant site which, in turn, provides a more favorable position to be filled up by metal ion than that in the hydration shell in bulk solution, as suggested by $Hoar^{(94)}$, the film is likely to form easily. The freshly formed film, still surrounded with a large amount of water, will change to a less hydrated structure

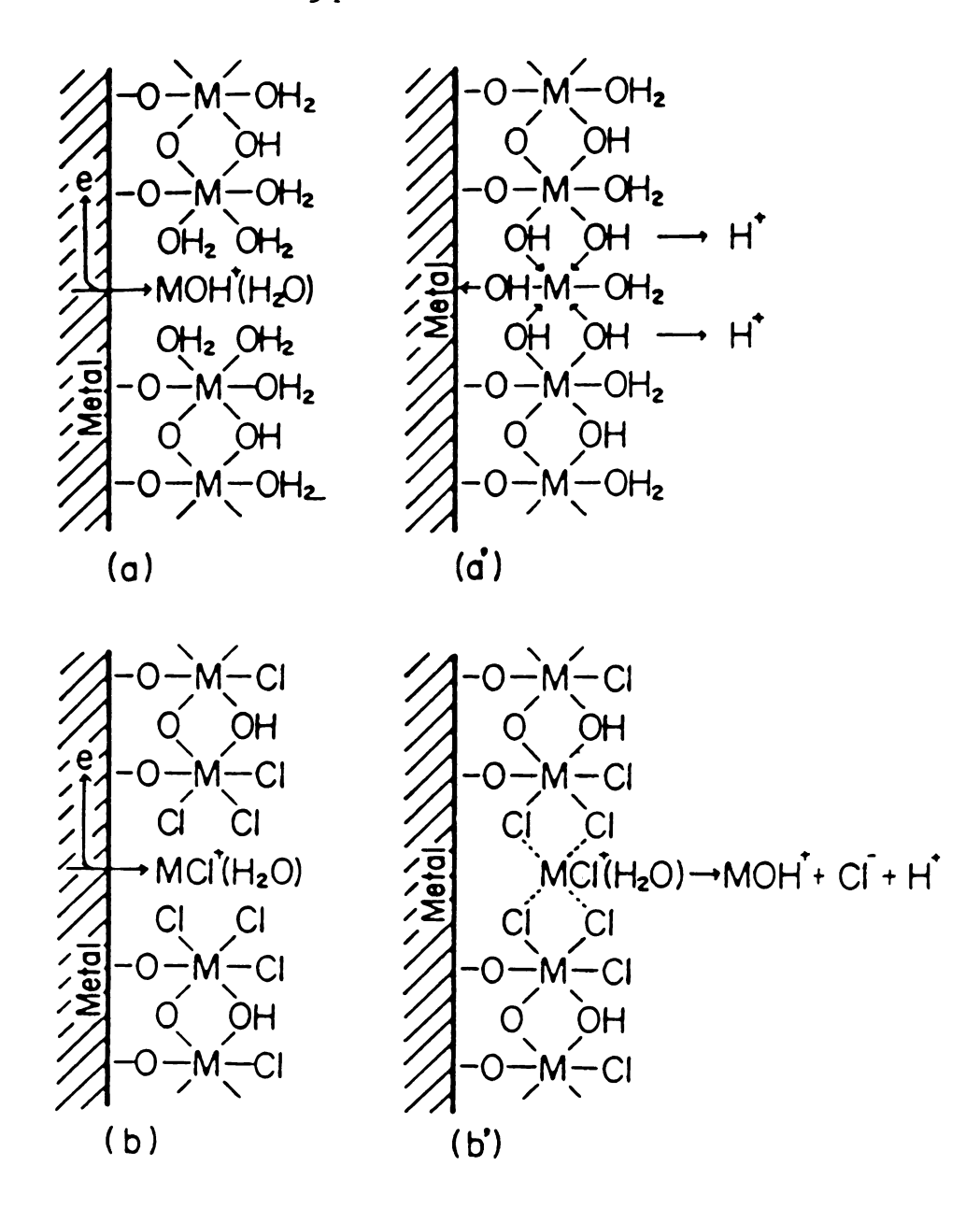


Figure 28. Schematic Models of the Passive Film in which bound water plays a dual function to help film formation and/or to be replaced by aggressive ions. (a) Metal ions dissolved are captured to form the film (a') due to the bridge of OH bond surrounding the site. (b) Chloride ions replacing water molecules inhibit the bridging action (b'), resulting the breakdown of the film.

with time. There exist three different types of bridge, H_2O-M-O_2H , HO-M-OH, O-M-O, depending on the degree in loss of proton. Thus the film might contain the various forms of bridge connecting between metal ions. If the proton is lost, the bridge changes to the oxide (O-M-O).

The breakdown of the film by aggresive anions, such as chloride at noble potentials, leads to nucleation and pit growth. If enough aggressive anions are accumulated and replace bound water, the repassivation is hindered leading to pit initiation (Figure 28-b and b'). In this model, bound water plays a critical role in assisting the repassivation. Among three types of oxygen bound, the M-OH type might be most effective for repassivation, whereas the M-OH₂ type is likely to be replaced easily by chloride ions. That is, the balance between repassivation and activation is a function of deprotonation.

On the other hand, the overall cathodic reaction in nearly neutral solutions may be the reduction of oxygen,

$$O_2 + 2H_2O + 4e^- ----> 4OH^-.$$
 (i)

Sodium nitrite was found to be an excellent inhibitor for aluminum in engine cooling systems $^{(94)}$ while it was found to accelerate the corrosion of aluminum in alkaline media $^{(95)}$. Sodium nitrite protects 7075-T6 Al alloy in

distilled water with good passivity at a tested concentration although the passive current density is increasing with the concentration (Figure 10). The protection given to aluminum alloy in distilled water by sodium direct result of action on the anodic nitrite is a dissolution/passivation procedures. Figure 29 shows a polarization diagram in aqueous system showing the anodic polarization curve with the development of passivity. The addition of an oxidizing inhibitor such as sodium nitrite shifts the cathodic polarization curve in the positive direction, thus stabilizing the corrosion potential in the passive region. The inhibition species are adsorbed on the metal surface and these adsorbed species develop the passivity, that is, insoluble oxide which protects the metal surface.

The presence of sodium chloride affects the inhibition of corrosion of 7075-T6 Al alloy. In the presence of sodium chloride, the inhibition of the corrosion depends on the ratio of nitrite to aggressive ion (Figure 12). Actually, the inhibition is not seen at low concentration of sodium nitrite but it is inhibited at higher concentration. It may be suggested that the passive film formed by the low concentration of sodium nitrite is still weak and ineffective against chloride attack without high concentration of inhibitor. The breakdown in the presence of insufficient nitrite is localized and severe, which can give rise to intense pitting and perforation. If no passivation results



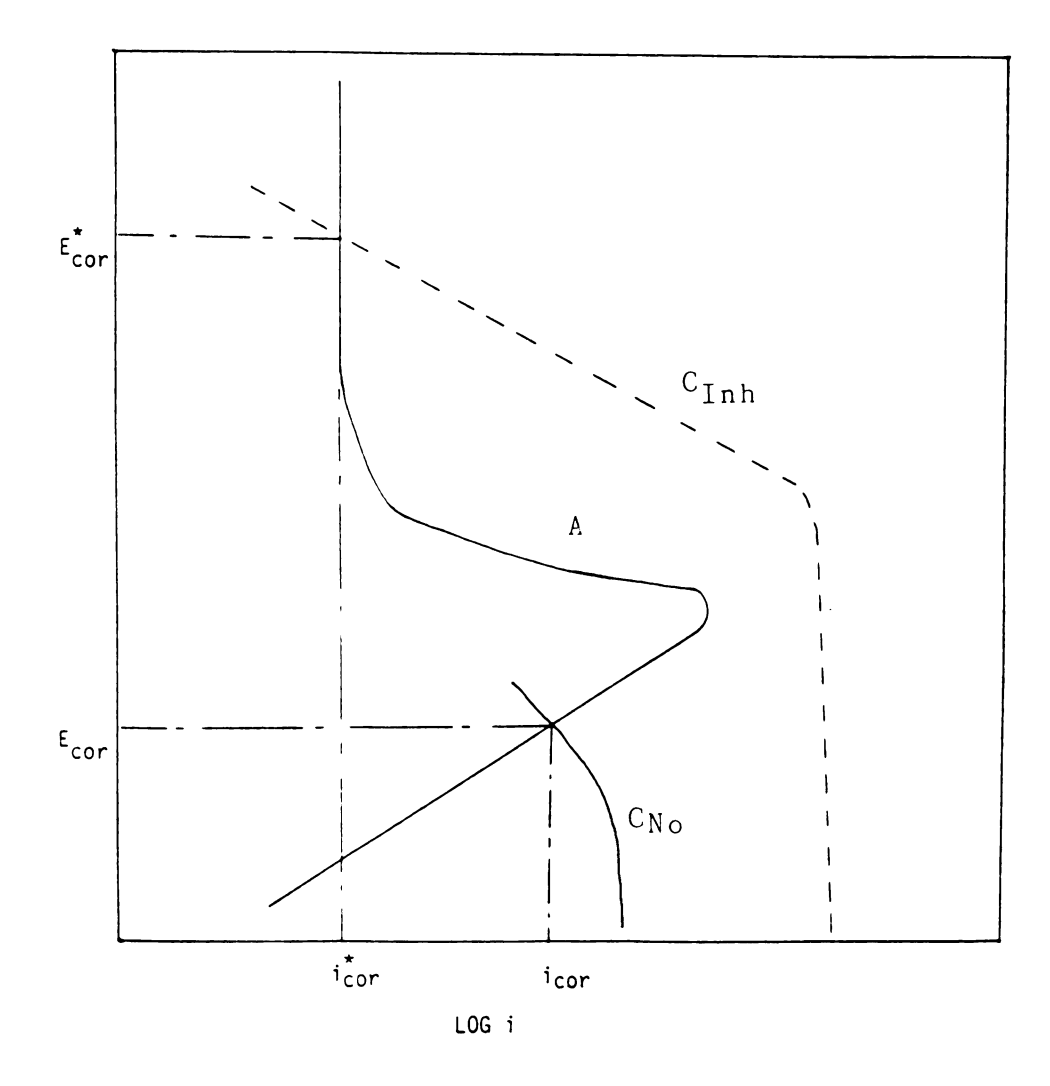


Figure 29. Schematic Polarization Diagram for Oxidizing Inhibitor.

at low concentration, as shown by the experimental results, metal dissolution increases and then the passive film becomes weak.

The inhibition process of sodium nitrite is accompanied by a shift in the corrosion potential in the positive direction, thus sodium nitrite is an anodic inhibitor. The inhibitor as sodium nitrite has no effect on the cathodic reaction where the current density increases with the concentration of sodium nitrite below -1.0 V as shown Figure 17. The cathodic reaction is

$$NO_2^- + 8H^+ + 6e^- --- > NH_4^+ + 2H_2^0.$$
 (J)

The corrosion in non-inhibited solutions of nitrite is usually accompanied by a marked rise in pH (from 6-7 to 9-10) during the experiment. This also is shown in the results of Mercer et al⁽³²⁾ who investigated the corrosion inhibitors for mild steel in neutral solution. The rise in pH is presumed to be due to cathodic reduction of nitrite ion to ammonia such as reaction (J) during the corrosion process. Cathodic reduction of low concentration of nitrite in chloride-containing solution could lead to eventual disappearance of nitrite from the solution: corrosion then should be of the type occurring in solutions free from inhibition. Increased corrosion rates in non-inhibiting

nitrites solutions have been reported by Sussman et $al^{(31)}$, Patterson and Jones⁽⁹⁶⁾, and Conoby et $al^{(98)}$.

The passive current density of a combination of sodium nitrite and borax is independent of concentration of borax (Figure 13). With the comparison in the case of sodium nitrite, it is increasing with the concentration. In the presence of sodium chloride, the effectiveness of the inhibition is eliminated even in the high concentration, although the pitting potential is increasing as the concentration is increasing (Figure 14 and Table 7). It is suggested that the film formed by these inhibitors still is unstable in the presence of sodium chloride as in the case of sodium nitrite. Bhansali et al (83) showed that crack growth rate is lowered by an order of magnitude after the addition of a combination of sodium nitrite and borax to chloride solution. These inhibitors have essentially eliminated environmentally assisted crack growth in chloride solutions.

The Lynch formulation shows results similar to those of the nitrite and borax combination. The pitting potential of the Lynch formulation is between that in the 0.5 wt.% borax and 0.1 wt.% borax (Figure 15). This results from the fact that 0.35 wt.% borax and 0.05 sodium nitrite of Lynch formulation is between the above concentration of borax. According to Khobaib et al⁽⁵⁸⁾, the borax-nitrite base

Table 7. Pitting potential of different test solutions with 0.1 wt.% NaCl

Concentration (wt.%)		Pitting potential (V vs SCE)
NaNO ₂	8.0	1.25
$NaNO_2 + Na_2B_4O_7$	(0.1,0.1)	-0.53
	(0.1,0.5)	-0.14
LYNCH	0.513	-0.48
NaNO ₃	0.5	-0.01
	1.0	1.08
	8.0	1.41
Na ₂ N ₂ O ₂	0.05	-0.50
	0.1	-0.63
	0.5	0.21
NH ₄ OH	0.05	-0.77
	0.1	-0.59
	0.5	-0.24
	1.0	-0.18

formulation provides protection to aluminum and steel, whereas this protection is lost with increasing concentration of chloride. They suggested that the passive film formed by the inhibition is weak and ineffective in the presence of chloride of high concentrations. But this inhibitor can give protection to aluminum and steel in high concentration of chloride if some surface active agents are added even in low concentration to this inhibitor formulation. It may be suggested that small additions of surface active agents interfere with the dissolution reaction by interacting synergistically with the passive film already by the inhibition formulation, which leads to a stronger and possibly thicker adsorbed protective film. Thus, the protective film formed by this inhibitor formulation with surface active agents slows down the dissolution reaction, as well as blocks aggressive anions from attacking the metal surface.

Once certain anions are adsorbed, they react chemically as shown by Augustynski $^{(98)}$ from the X-ray Photoelectron Spectroscopy(XPS). The results shows that NO $_3$ is reduced to NH $_4$ and the presence of nitrate retards the adsorption of chloride. It also is reported that nitrate is reduced by elemental aluminum in alkaline solution $^{(99)}$,

$$8A1^{\circ} + 3NO_{3}^{-} + 5OH^{-} + 18H_{2}O ----->$$

$$8Al(OH)_4 - 3NH_3$$

and the reduction potential for the couple NO_3^-/NH_4^+ is 0.47 $V^{(100)}$.

It has been confirmed $^{(61)}$ that the formation of NH $_3$ results from the chemical reaction between NO $_3$ and the aluminum metal. When a solution of NaNO $_3$ was brought into contact with aluminum metal, the formation of ammonia could be recognized after 16 hours by ammonia odor. Upon shaking the suspension vigorously, the formation of NH $_3$ was quickly accelerated within a few minutes.

It was reported ⁽⁶²⁾, ⁽¹⁰¹⁾ that NH₃ was formed on rapidly corroding aluminum alloys 2024 and 7075 in certain mixtures of chloride and nitrate, whereas aluminum alloy 1199, essentially pure aluminum, didn't show the synergistic effect of chloride accelerating film dissolution. This resulted from the presence of Cu and Zn as alloying elements which acted as local alkaline cathodic site. Chemical reactions between NH₃ produced by reduction of NO₃ and intermetallic compound are

$$CuAl_2 + 4NH_3 = Cu(NH_3)_4^{2+}$$
 in alloy 2024

$$K_{instability} = 2.4 \times 10^{-13}$$

$$MgZn_2 + 4NH_3 = Zn(NH_3)_4^{2+}$$
 in alloy 7075
 $K_{instability} = 3.46 \times 10^{-10}$.

Both complexes are very soluble and will accelerate the attack. The existence of a specific concentration of mixture of chloride and nitrate in which corrosion was accelerated was because of the competition between inhibition with nitrate and the acceleration with chloride.

Figure 20 shows the effectiveness depending on the concentration of sodium nitrate in the chloride-containing solution. As the concentration of nitrate is increasing, the inhibition among the competition between inhibition and acceleration becomes dominated and the pitting potential is increasing (Table 7). The concentration of 0.1 wt.% NaNO₃ in the chloride-containing solution shows the synergistic effect as explained above. The pitting potential has been explained in terms of Cl penetrating an oxide film which covers the metal surface (102), (103) or in terms of competitive adsorption of Cl and oxygen for sites on the metal surface (52), (104), which is dependent upon the oxide film. The thicker oxide film, the smaller is the electric film impelling Cl to penetrate it and the longer is the diffusion path of Cl from electrolyte to metal surface.

Bohni and $Uhlig^{(51)}$ also noted that $NaNO_3$ addition to NaCl solutions moved the pitting potential in noble direction corresponding to improved corrosion resistance and the relationship between chloride activity and inhibiting nitrate activity followed the equation

$$log(Cl^{-}) = 0.65log(NO_{3}^{-}) - 0.78.$$

Challender (105) also showed that the rate of reduction of nitrate is related directly to the concentration required to achieve passivation for Al alloy.

There seems to be no threshold for chloride concentration below which pitting would never occur and the addition of inhibition, NO_3 would delay but not prevent the onset of pitting as discussed by Berzins, et al⁽⁴⁵⁾. They showed that the delay time before the onset of pitting is logarithmically related to inhibitor concentration.

Temperature as might be expected has considerable influence on corrosion rate. Figures 30 and 31 show that the current density logarithmically is dependent upon the temperature in the solution of sodium nitrate and sodium nitrite although the temperature dependence of sodium nitrite is more scattered than that of sodium nitrates. These figures give the slopes which are related to the

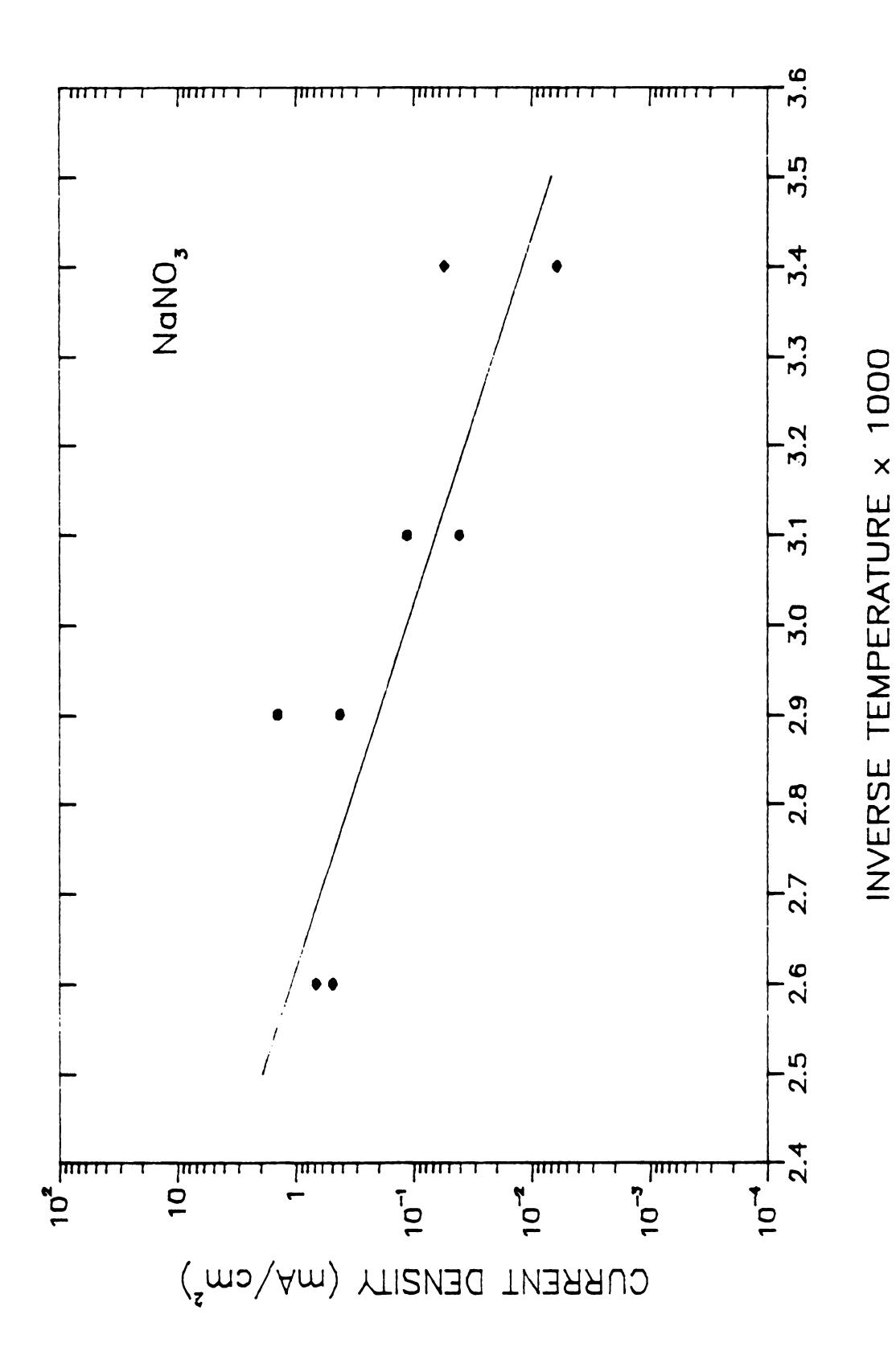


Figure 30. Dependence of the Current Density on Temperature in Sodium Nitrate.

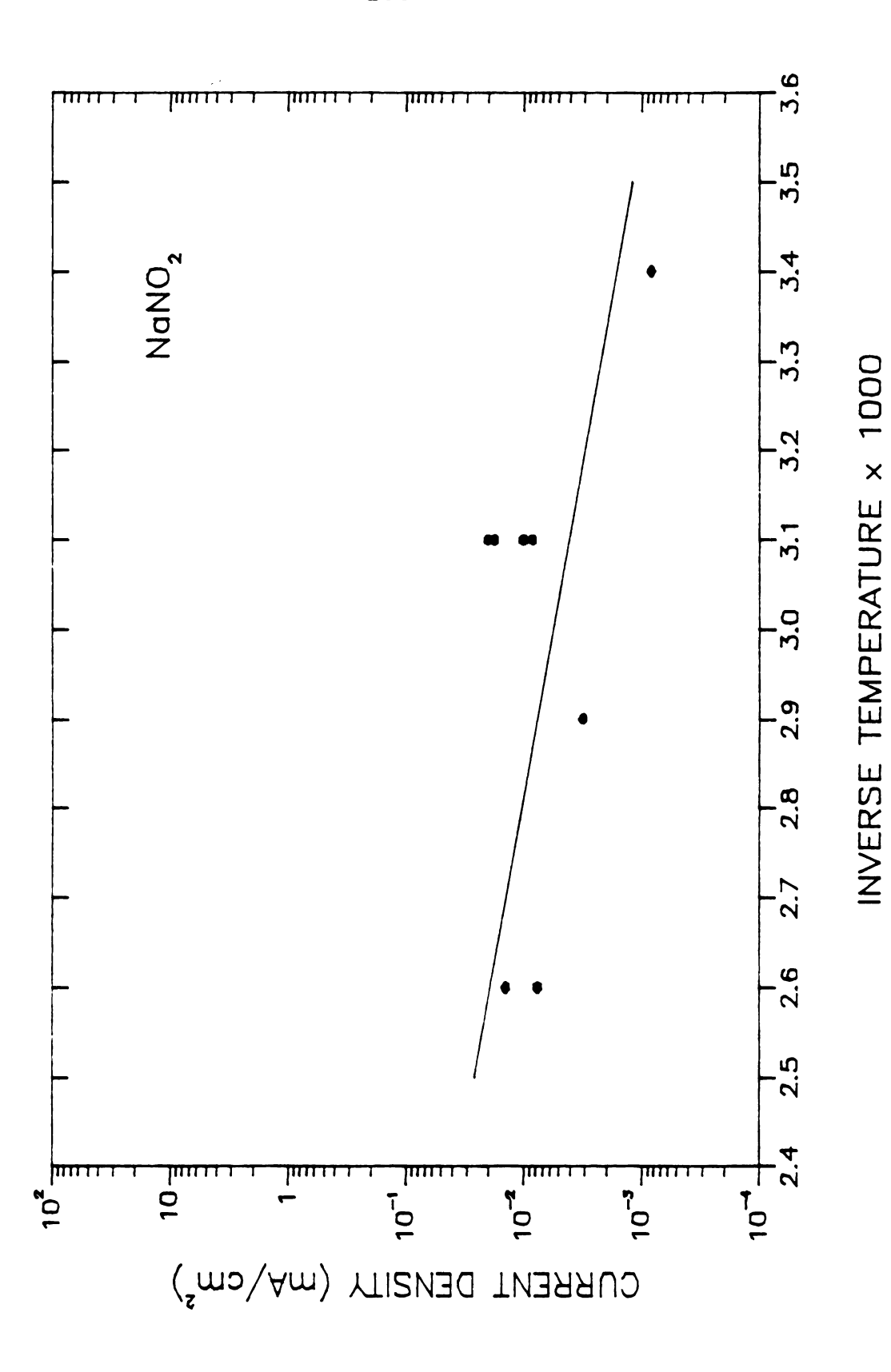


Figure 31. Dependence of the Current Density on Temperature in Sodium Nitrite.

Arrehenius activation energy 2.68 kcal/mol for nitrite and 4.88 kcal/mol for nitrate.

Hyponitrite has both reducing and oxidizing properties but the reducing properties predominate. As indicated by Figure 22, the hyponitrite has a strong passivating effect on 7075-T6 Al alloy. Although the passive current density of hyponitrite is larger than that of nitrite, the region of passivity is wider and the pitting potential is higher (Table 7). This results from the larger reduction potential with comparison between potential of nitrite and hyponitrite. The passivity breaks down in the chloride-containing solution (Figure 23), but hyponitrite has the strongest effectiveness of inhibition among nitrite, nitrate and hyponitrite when the inhibition effectiveness is compared at the same concentration, i.e., the hyponitrite has the strongest passivity film against chloride attack.

It has been reported $^{(106)}$ that dry ammonia has no action on aluminum even at elevated temperature. When ammonia is moist or in solution as ammonium hydroxide, the corrosion rate is low for all concentrations at temperatures up to $120^{\circ}F^{(107)}$. Ammonium hydroxide shows the strong effectiveness in passivation of 7075-T6 Al alloy, although the passive current density is increasing with the concentration because a thin protective oxide film forms after exposure to ammonium ion and prevents further attack (Figure 24). The region of passivity is as wide as the

sodium hyponitrite (Table 7). Results similar to those of sodium hyponitrite are obtained in chloride-containing solution (Figure 25). Thus, aluminum is typically used for ammonia refrigeration tubing, storage vessels, sprays and molds in contact with ammoniacal rubber latex. Aluminum equipment also is used widely in contact with ammonium bicarbonate, ammonium carbonate, urea and ammonium nitrate.

VI. Conclusion

Generally, the inhibitors used in this study i.e., NaNO_2 , Lynch Formulation, combination of NaNO_2 and $\operatorname{Na}_2\operatorname{B}_4\operatorname{O}_7$, NaNO_3 , $\operatorname{Na}_2\operatorname{Na}_2\operatorname{O}_2$, $\operatorname{NH}_4\operatorname{OH}$ show good passivation on 7075-T6 Al alloy in distilled water. In the presence of chloride, the passivity is dependent on the concentration of the inhibitor in the solution which determines the competitive action between the inhibitor and the aggressive ion. The inhibitive efficiency of oxyanions of nitrogen based on the pitting potential is in the decreasing order of: $\operatorname{Na}_2\operatorname{Oa}_2$ > NH_4^+ > NOa_3^- > Lynch Formulation > combination of NOa_2^- and BaOa_3^2 > NOa_3^2 .

The current density depends logarithmically upon the temperature in the solution of sodium nitrite and sodium nitrate, the acivation energies of which is 2.68 kcal/mol and 4.88 kcal/mol, respectively.

LIST OF REFERENCES

- 1. C. Schonbein, Pogg. Ann., 44, 73(1838)
- 2. A. Finklestein, Z. Physik. Chem., 39, 91(1902)
- 3. W.J. Muller, Z. Elektrochem., 10, 518(1904)
- 4. M. Le Blanc, Z. Elektrochem., 6, 472(1900); Trans.

 Faraday Soc., 9, 255(1913)
- 5. Gmelin, Teil 59A, "Handbuch der Anorganischen Chemie", P313, Berlin, 1929-1932
- 6. F. Haber, Z. Elektrochem., 10, 697(1904)
- 7. H. Heathcote, <u>J. Soc. Chem. Ind. London, 26</u>, 899(1907)
- 8. U.R. Evans, <u>J. Chem. Soc. London</u>, 1020(1927)
- 9. C. Fredenhagen, <u>Z. Physik. Chem., 43</u>, 1(1903); ibid, 63,1,(1908)
- 10. I. Langmuir, Trans. Electrochem. Soc., 29, 260(1916)
- 11. H.H. Uhlig, <u>Corrosion Sci.</u>, 7, 325(1967)
- 12. K. Kudo, T. Shibata, G. Okamoto and N. Sato,

 Corrosion Sci., 8, 809(1968)
- 13. H. Yolken, J. Kruger and J. Calvent, <u>Corrosion Sci.</u>,
 8, 103(1968)
- 14. G. Okamoto and T. Shibata, Nature, 206, 1350(1965)
- 15. B. Kabanov, R. Burstein and A. Frumkin, <u>Discuss</u>

 <u>Faraday Soc.</u>, 1, 259(1947)
- 16. L.L. Shreir, "Corrosion", 2nd ed., Butterworths, London, 1976

- 17. Sheldon w. Dean, Jr, Richard Derby and Glenn T. Van

 Dem Bussche, <u>Materials Performance</u>, Dec., 47(1981)
- 18. Morris Cohen, <u>Corrosion</u>, <u>32</u>, 461(1976)
- R. Pyke and M. Cohen, <u>J. Electrochem. Soc.</u>, 93,
 63(1948)
- 20. J.E.O. Mayne and M.J. Pryor, <u>J. Chem. Soc.</u>,
 1831(1949)
- 21. M. Cohen, J. Phys. Chem., 56, 451(1952)
- 22. M. Cohen, <u>J. Electrochem. Soc.</u>, 121, 191(1974)
- 23. I.L. Rozenfeld, <u>Corrosion</u>, <u>37</u>, 371(1981)
- 24. I.L. Rozenfeld, "Corrosion Inhibitors", R. and H. Hardin, transl., McGraw-Hill, New York, 1981
- 25. I.L. Rozenfeld and I.K. Marshakov, <u>Corrosion</u>, 20, 115t(1964)
- 26. A. Marshall, Corrosion, 37, 214(1981)
- 27. V.M. Ledovskikh, Z. Metallov. 19, 9, 84(1983)
- 28. R.A. Legault and M.S. Walker, <u>Corrosion</u>, 20, 282(1964)
- 29. A. Wachter and S. Smith, <u>Ind. and Eng. Chem., 35</u>, 358(1943)
- 30. M. Cohen, J. Electrochem. Soc., 93, 26(1948)
- 31. S. Sussman, O. Nowakowski, and J. Constantino, <u>Ind.</u>
 and Eng. Chem., 51, 581(1959)
- 32. A.D. Mercer, I.R. Jenkins and J.E. Rhoades-Brown,

 Bri. Corrosion J., 3, 136(1968)
- 33. R.T. Foley, <u>Corrosion</u>, <u>26</u>, 58(1970)
- 34. M. Maeda, Nature, 44, 557(1957)

- 35. S. Matsuda and H.H. Uhlig, <u>J. Electrochem. Soc., 111</u>, 156(1964)
- 36. Y.N. Mikhailovskii, V.M. Popova and T.I. Sokolva, Z. Metallov., 19, 707(1983)
- 37. E. McCafferty, "Corrosion Control by Coatings", H. Leiheiser, Jr. ed., Science Press, Princeton, New Jersey, 1979
- 38. E. McCafferty, J. Electrochem. Soc., 126, 385(1979)
- 39. B.W. Samuels, K. Sotoudeh and R.T. Foley, <u>Corrosion</u>, 37, 92(1981)
- 40. W. Vedder and D.A. Vermilyea, <u>Trans. Faraday Soc.</u>, <u>554</u>, 561(1964)
- 41. D.A. Vermilyea and W. Vedder, <u>General Electric Memo</u>,
 MO-68-0551 (April, 1968)
- B. Verkerk, <u>Int. Conf. Radioisotopes Sci. Res., 1</u>, 503(1957)
- 43. V.T. Belov, <u>Zashch. Met.</u>, 475(1968)
- 44. E. Herczynska and K. Proszynska, <u>J. Inorg. Nucl.</u>
 Chem., 26, 1429(1964)
- 45. A. Berzins, R.T. Lowson and K.J. Mirams, <u>Aust. J.</u>
 Chem., 30, 1891(1977)
- 46. Z.A. Foroulis and Thubrikar, <u>J. Electrochem. Soc.</u>, <u>122</u>, 10(1975)
- S. Dallek and R.T. Foley, <u>J. Electrochem. Soc.</u>, <u>123</u>,
 12, 1775(1976)
- 48. T.H. Nguyen and R.T. Foley, <u>J. Electrochem. Soc.</u>, <u>129</u>, 27, (1982)

- 49. R.T. Foley and T.H. Nguyen, <u>J. Electrochem. Soc.</u>, <u>129</u>, 464(1982)
- 50. K.F. Locking and J.E.O. Mayne, <u>J. Appl. Chem.</u>, <u>11</u>, 170(1961)
- 51. H. Bohni and H.H. Uhlig, <u>J. Electrochem. Soc., 116</u>, 906(1962)
- 52. H.P. Leckie and H.H. Uhlig, <u>J. Electrochem. Soc.</u>, 113, 1262(1966)
- 53. J.T. Bregman and D.B. Boies, <u>Corrosion</u>, <u>14</u>, 275(1958)
- 54. D.R. Robitaille, <u>Materials Performance</u>, <u>15</u>, 11(1976)
- 55. A. Weisstuch and C.E. Schell, Corrosion, 28, 299(1972)
- 56. A.D. Mercer and F. Formwell, <u>J. Appl. Chem.</u>, 9, 577(1959)
- 57. J.G.N. Thomas and T.J. Nurse, <u>Bri. Corrosion J., 2</u>, 13(1967)
- 58. M. Khobaib, L. Quakenbush and C.T. Lynch, <u>Corrosion</u>, 39, 253(1983)
- 59. M. Khobaib, "Bilge Inhibitors", AFWAL-TR-81-4186,
 Materials Laboratory, Wright-Patterson AFB, Ohio, 1982
- 60. J. Green and D.B. Boies, "Corrosion Inhibitor

 Composition for Aqueous Liquids", U.S. Patent No. 2,

 815, 328, 3, December (1957)
- 61. T.H. Nguyen and R.T. Foley, <u>J. Electrochem. Soc.</u>,

 127, 2563(1980)
- 62. A.M. McKissick, A.A. Adam and R.T. Foley, <u>J.</u>

 Electrochem. Soc., 117, 1459(1970)

- 63. P.J. Anderson and M.E. Hocking, <u>J. Appl. Chem.</u>, 8, 352(1958)
- 64. T. Moeller, "Inorganic Chemistry An Advanced Text Book", John Wiley, New York, 1952
- 65. H. Block, "Mellor's Comprehensive Treatise on Inorganic and Theoretical Chemistry", Vol. III, Suppl. II, Part II, John Wiley & Sons Inc., Section XXXII, P366
- 66. W.L. Jolly, "Inorganic Chemistry of Nitrogen", W.A. Benjamin Inc., New York, 1964
- 67. M.N. Hughes and G. Stedman, <u>J. Chem. Soc. London</u>, 1239(1963)
- 68. W.M. Lattimer and H.W. Zimmerman, <u>J. Am. Chem. Soc.</u>, 61, 1550(1939)
- 69. D.D. Wagman, W.H. Evans, V.B. Parker, I. Halow, S.M. Bailey and R.H. Schumm, "Selected Values of Chemical Thermodynamic Properties", NBS Technical Note 270-3, Washington(1968)
- 70. C.C. Addison, G.A. Gamlen and R. Thompson, <u>J. Chem.</u>
 Soc., Vol. 338(1952)
- 71. M.N. Huges, <u>Quart. Rev.</u>, 22, 1(1968)
- 72. D.J. Miller, C.N. Polydoropoulos and D. Watson, J. Chem. Soc., Vol. 687(1960)
- 73. L. Kuhn and E.R. Lippincott, <u>J. Amer. Chem. Soc., 78</u>, 1820(1956)
- 74. M.N. Huges, <u>J. Inorq. Nuclear Chem.</u>, 29, 1376(1967)

- 75. G.E. Mcgraw, D.L. Bernitt and I.C. Hisatsune,

 Spectrochim. Acta, 23, A, 25(1967)
- 76. "Advanced Inorganic Chemistry A Comprehensive Text", Cotton and Wilkinson, Fourth ed.,
 Interscience, John Wiley & Sons, 1980
- 77. Alcoa Technical Center, Aluminum Company of America
- 78. "Metals Handbook", 8th ed., Vol. 1, P948, ASM(1961)
- 79. "Organic Synthesis, Collective", Vol. 1, New York-London, P539, 1941
- 80. "Handbook of Preparative Inorganic Chemistry", P495
- 81. L.F. Fieser, "Experiments in Organic Chemistry", P419, New York, 1941
- 82. H. Omura, "Effect of Multi-Functional Inhibitors on the Electrochemistry with a Corrosion Crack", Ph.D. Thesis, Michigan State University, 1984
- 83. K. J. Bhansali, C.T. Lynch, F. Vahldiek and R. Summitt, "Effect of Multifunctional Inhibitors on Crack Propagation Rate of High Strength Steel in Corrosive Environments", Conf. Effect of Hydrogen on Mechanical Behavior of Materials, Moran, WY., 7-11 Sept., 1975
- 84. C.T. Lynch, F. Vahldiek, K.J. Bhansali and R. Summitt, "Inhibition of Environmentally Enhanced Crack Growth Rates in High Strength Steels", Symp. Environment Sensitive Fracture of Engineering Materials, AIME Meeting, Chicago, IL, 26 Oct. 1977
- 85. H.P. Godard, <u>Materials Performance</u>, July, 7(1981)

- 86. K. Videm, Kjeller Report No. KR-149, Institute for Atommenergi, 1974
- 87. J.A. Richardson and G.C. Wood, <u>J. Electrochem. Soc.</u>, <u>120</u>, 193(1973)
- 88. J.A. Richardson and G.C. Wood, <u>Corrosion Sci., 10</u>, 313(1970)
- 89. W.J. Bernard and J.J. Randall, Jr., <u>J. Electrochem.</u>
 Soc., 108, 822(1961)
- 90. H.B. Konno, S Kobayashi, H. Takahashi and M. Nagayama, Corrosion Sci., 22, 913(1982)
- 91. T. Hagyard, W.B. Earl and M.J. Pryor, <u>Trans. Faraday</u>
 Soc., <u>57</u>, 2288(1961)
- 92. S. Dallek and R.T. Foley, <u>J. Electrochem. Soc., 125</u>, 731(1978)
- 93. G. Okamoto and T. Shibata, "Passivity of Metals",
 R.P. Frankenthal and J. Kruger Eds., Electrochemical
 Society, Pennington, New Jersey, P660, 1978
- 94. L.C. Rowe, Corrosion 13, 756(1957)
- 95. M.N. Desai, S.M. Desai, M.H. Gandhi and C.B. Shab,

 Anti-Corrosion, April, 8(1971), Reference 50
- 96. W.S. Patterson and A.W. Jones, <u>J. Appl. Chem. London</u>, <u>2</u>, 273(1952)
- 97. J.F. Conoby and T.M. Swalin, Mater. Prot., April, 55(1967)
- 98. J. Augustynski, "Passivity of Metals", R.P. Frankenthal and J. Kruger Eds., Electrochemical Society, Pennington, New Jersey, P989, 1978

- 99. P.C.L. Thorne and E.R. Roberts, "Fritz Ephraim
 Inorganic Chemistry", 5th ed., Gurney and Jackson,
 London, England, P620, 1949
- 100. W.L. Latimer, "Oxidation Potentials", 2nd ed.,
 P104, Prentice-Hall Inc. Englewood Cliffs, New
 Jersey(1952)
- 101. A.A. Adams, K.E. Eagle and R.T. Foley, <u>J.</u>

 <u>Electrochem. Soc., 119</u>, 1692(1072)
- 102. M. Streicher, <u>J. Electrochem. Soc.</u>, 103,375(1956)
- 103. T. Hoar, D. Mears and G. Rothwell, <u>Corrosion Sci., 5</u>, 279(1965)
- 104. Y. Kolotyrkin, <u>Corrosion</u>, 19, 261t(1963)
- 105. L.H. Challender, Engineering, 120, 340(1925)
- 106. E.D. Verink Jr., Chem. Eng., 57, 111(1950)
- 107. F.L. LaQue and H.R. Copson, "Corrosion Resistance of Metals and Alloys", 2nd ed., Reinhold Publishing Corp., New York, P205(1963)





